LEVEL II

RADC-TR-79-101
Final Technical Report
May 1979

OVERLAPPED SUB-ARRAY SCANNING ANTENNA STUDY

Guidance Systems, Inc.

G. Ploussios

pcm

APPROVED FOR PUBLIC RELEASE; DISTRIBUTION UNLIMITED

ROME AIR DEVELOPMENT CENTER
Air Force Systems Command
Griffiss Air Force Base, New York 13441

DISCLAIMER NOTICE

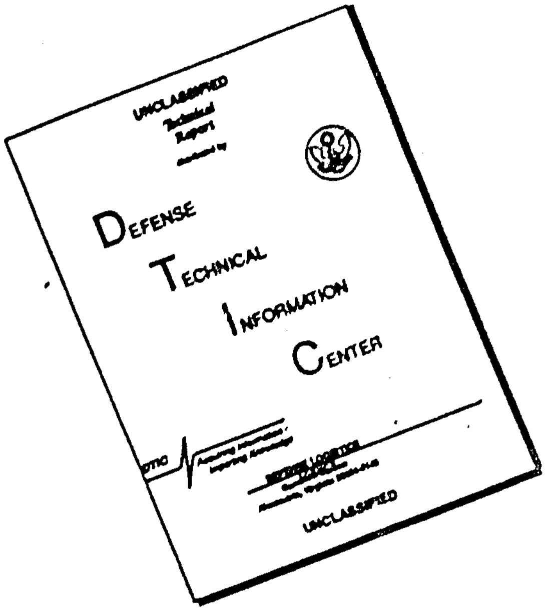

THIS DOCUMENT IS BEST QUALITY AVAILABLE. THE COPY FURNISHED TO DTIC CONTAINED A SIGNIFICANT NUMBER OF PAGES WHICH DO NOT REPRODUCE LEGIBLY.

This report has been reviewed by the RADC Information Office (OI) and is releasable to the National Technical Information Service (NTIS). At NTIS it will be releasable to the general public, including foreign nations.

RADC-TR-79-101 has been reviewed and is approved for publication.

APPROVED: Hermann Ehrenspeck

HERMANN EHRENSPECK
Project Engineer

APPROVED: Walter Rotman

WALTER ROTMAN
Chief, Antennas & RF Components Branch
Electromagnetic Sciences Division

APPROVED: Allan C. Schell

ALLAN C. SCHELL
Chief, Electromagnetic Sciences Division

FOR THE COMMANDER: John P. Huss

JOHN P. HUSS
Acting Chief, Plans Office

UNCLASSIFIED

SECURITY CLASSIFICATION OF THIS PAGE (When Data Entered)

REPORT DOCUMENTATION PAGE		READ INSTRUCTIONS BEFORE COMPLETING FORM
1. REPORT NUMBER RADC-TR-79-101	2. GOVT ACCESSION NO.	3. RECIPIENT'S CATALOG NUMBER
4. TITLE (and Subtitle) OVERLAPPED SUB-ARRAY SCANNING ANTENNA STUDY		5. TYPE OF REPORT & PERIOD COVERED Final Technical Report
		6. PERFORMING ORG. REPORT NUMBER
7. AUTHOR(s) G. Ploussios		8. CONTRACT OR GRANT NUMBER(s) F19628-78-C-0069
9. PERFORMING ORGANIZATION NAME AND ADDRESS Guidance Systems Inc. 4 Hackney Circle Andover MA 01810		10. PROGRAM ELEMENT, PROJECT, TASK AREA & WORK UNIT NUMBERS 62702F 46001438
11. CONTROLLING OFFICE NAME AND ADDRESS Deputy for Electronic Technology (RADC/EEA) Hanscom AFB MA 01731		12. REPORT DATE May 1979
		13. NUMBER OF PAGES 70
14. MONITORING AGENCY NAME & ADDRESS(if different from Controlling Office) Same		15. SECURITY CLASS. (of this report) UNCLASSIFIED
		15a. DECLASSIFICATION/DOWNGRADING SCHEDULE N/A

16. DISTRIBUTION STATEMENT (of this Report)

Approved for public release; distribution unlimited.

17. DISTRIBUTION STATEMENT (of the abstract entered in Block 20, if different from Report)

Same

18. SUPPLEMENTARY NOTES

RADC Project Engineer: Hermann Ehrenspeck (EEA)

19. KEY WORDS (Continue on reverse side if necessary and identify by block number)

Phased array antennas
Scanning antennas
Limited scan antennas
Radar antenna systems
Low sidelobe antennas
Multiple beam arrays

20. ABSTRACT (Continue on reverse side if necessary and identify by block number)

This report refers to an investigation of new phased array techniques using overlapping multiple beam elements. It is shown that this technique, ~~which was conceived by GS, Inc.~~ can be applied to a wide variety of electronically scanned system requirements. Two designs, one for limited scan and the other for wide angle scan with a minimum number of elements and phase shifters were selected for the reported computer analysis. The results indicate extremely low sidelobe levels over most of the angular sector while limiting → next page
(Cont'd)

DD FORM 1 JAN 73 1473

UNCLASSIFIED

SECURITY CLASSIFICATION OF THIS PAGE (When Data Entered)

S/C JOB

393 480

Item 20 (Cont'd)

+ or - 10 deg.

the close-in sidelobes to no more than -20 dB and grating lobe levels to peak values of about -14 dB for some scan locations. The limited scan design utilizes 18 eight-port Bulter matrices, 18 phase shifters, and 9 SP2T switches to achieve 20 BW's of a ± 10° scan. The wide-angle design provides 90 BW's of scan (±45°) with 26 eight-port matrix elements, 26 phase shifters and 26 SP4T switches. The analysis of the new scan array technique indicates that the array performance can be further improved at the cost of additional elements and element complexity.

+ or - 45 deg.

TABLE OF CONTENTS

LIST OF ILLUSTRATIONS

LIST OF ILLUSTRATIONS (cont'd)

Figure No.

EVALUATION

1. This report is the final report on the contract. It covers a theoretical investigation of a phased array technique using overlapped multiple-beam elements. The limited study effort examined the general relationship between the system parameters. Design curves are presented relating these parameters to the performance and complexity of the system. In general it is shown that the number of phase shifters required in this antenna system is much lower than the number of beamwidths of scan. The results indicate that extremely low sidelobe levels can be achieved over most of the angular sector with the close-in sidelobes limited to no more than -20 dB and grating lobe levels to peak values of about -14 dB for a few scan locations. The pattern performance can be further improved at the cost of additional elements.

2. This effort was supported under project 4600, task 14. The results obtained are applicable to tactical and space based radar antennas because they illustrate potential low cost techniques for scanning array implementation.

Hermann Ehrenspeck
HERMANN EHRENSPECK
Contract Monitor

I. PROGRAM OBJECTIVES

The objective of the subject study program is to analyzé a new array technique using overlapped multiple-beam elements that are arrayed and phased to provide a scannable narrow beam with a minimum number of phase shifters. In addition to studying the array parameter relationships versus performance and cost, a set of parameters are to be selected to demonstrate performance via computer simulation. The designs to be simulated are:

Limited Scan

Beamwidth	-	1°
Scan coverage	-	$\pm 10°$

Wide Angle Scan

Beamwidth	-	1°
Scan coverage	-	$\pm 45°$

II. STUDY PROGRAM SUMMARY

A new array technique* incorporating a number of overlapped large multibeam elements has been examined. The technique results in a substantial reduction in numbers of phase shifters by providing a step scan element pattern that is selected via a SPMT switch.

The number of parameters available to the designer in selecting the best design for a given specification include:

1. Number of multiple-beam elements/phase shifters
2. Element overlap factor
3. Array distribution
4. Element size
5. Element pattern
6. Element step scan design.

The limited study effort described in this report examined the general relationships between these parameters and system performance. Design curves are presented relating these parameters to system performance and complexity. In general, it is shown that the number of phase shifters required in this system is much less than the number of BW's of scan.

A set of parameters were selected for examination in greater detail for limited scan (± 10°, 1°BW) and wide angle scan (±45°, 1°BW) applications. The results of this examination indicated satisfactory performance for a given set of performance requirements and pointed out areas that could be improved upon by selecting other system parameters.

* Patent application filed.

Antenna patterns were computer simulated for a minimum number of components design. The system parameters were:

Limited Scan

BW	-	1°
Scan	-	±10°
# elements	-	18
# phase shifters	-	18
# of switches	-	9 (SP2T)
Sidelobes	-	<-20 dB close-in
		<-40 dB beyond ±25°
Grating lobe	-	typically -14 dB to -20 dB
Element type	-	8 port Butler Matrix
Array Efficiency	-	-3.2 dB

Wide Angle Scan

BW	-	1°
Scan	-	±45°
# elements	-	26
# phase shifters	-	26
# switches	-	26 (S°4T and SP3T)
Sidelobes	-	<-20 dB close-in
		<-40 dB beyond ±25°
Grating lobe	-	typically -14 dB to -20 dB
Element type	-	8 port Butler Matrix
Array Efficiency	-	-3.2 dB

The following sections cover the relationship between the design parameters and system performance and then the detail computer simulation results for the parameter subset selected. Evaluation of the designs studied includes performance sensitivity to component errors and cost/performance trade offs.

III. ARRAY DESIGN

A. Principle of Operation

The array approach examined in this study is based upon arraying and phasing elements that are electrically large, i.e., greater than one wavelength. Each of these elements produces a narrow beam, the direction of which is selected and determined by means of a multiple-beam (MB) network or lens. In order to avoid grating lobes, the spacing between elements must be less than an element width, i.e., the elements must overlap. This is realized by overlapping the multiple-beam matrices (lens) and coupling the overlapped outputs through P:1 combiners (P is the maximum number of matrices overlapped at any point on the array) to a set of common radiators as illustrated in Figure III-1. The array is scanned by adjusting the N phase shifters feeding the large element networks (lens) using phase shift values identical to that required of a conventional array with interelement spacing equal to A/P.

$$\psi_n = \frac{2\pi(n-1)}{\lambda} \frac{A}{P} \sin \theta_o \qquad \text{(III-1)}$$

The array pattern is determined by the product of the array factor and the element pattern. A typical case is illustrated in Figure III-2. The array factor grating lobe structure scans with the desired main beam. In order to avoid high grating lobes in the array pattern, the array scan must be restricted to angles that limit the grating lobe location to angles that correspond to low-element pattern values. This is possible when one half the element null width is less than the grating lobe spacing; i.e.,

$$\sin^{-1} \left(\frac{P\lambda}{A}\right) > \sin^{-1} \left(\frac{K\lambda}{A}\right) \qquad \text{(III-2)}$$

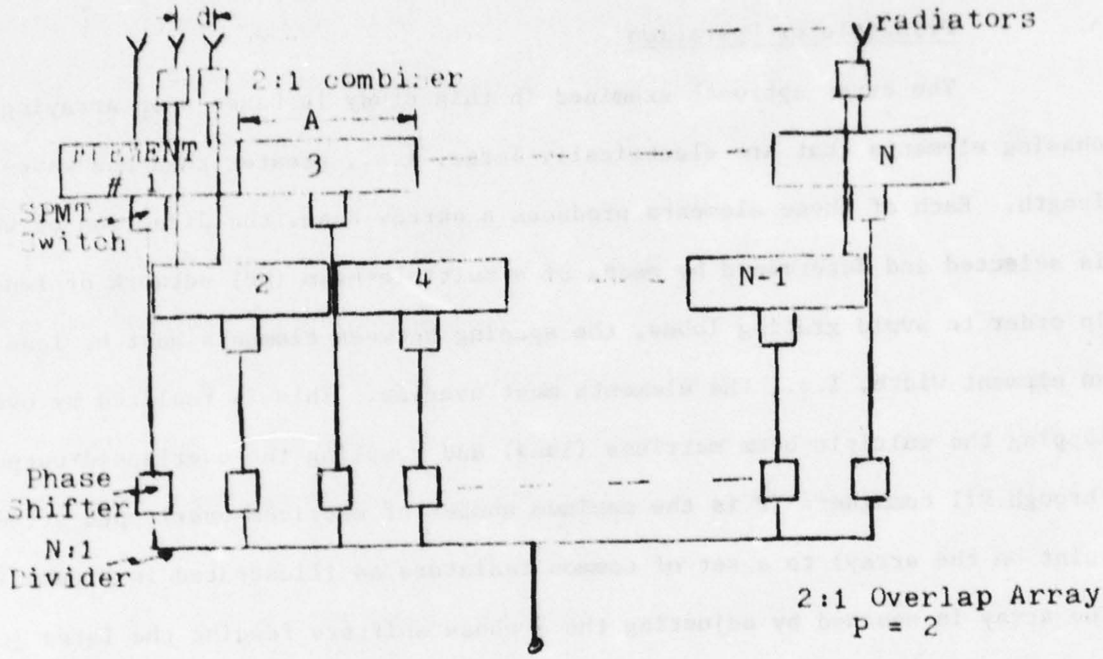

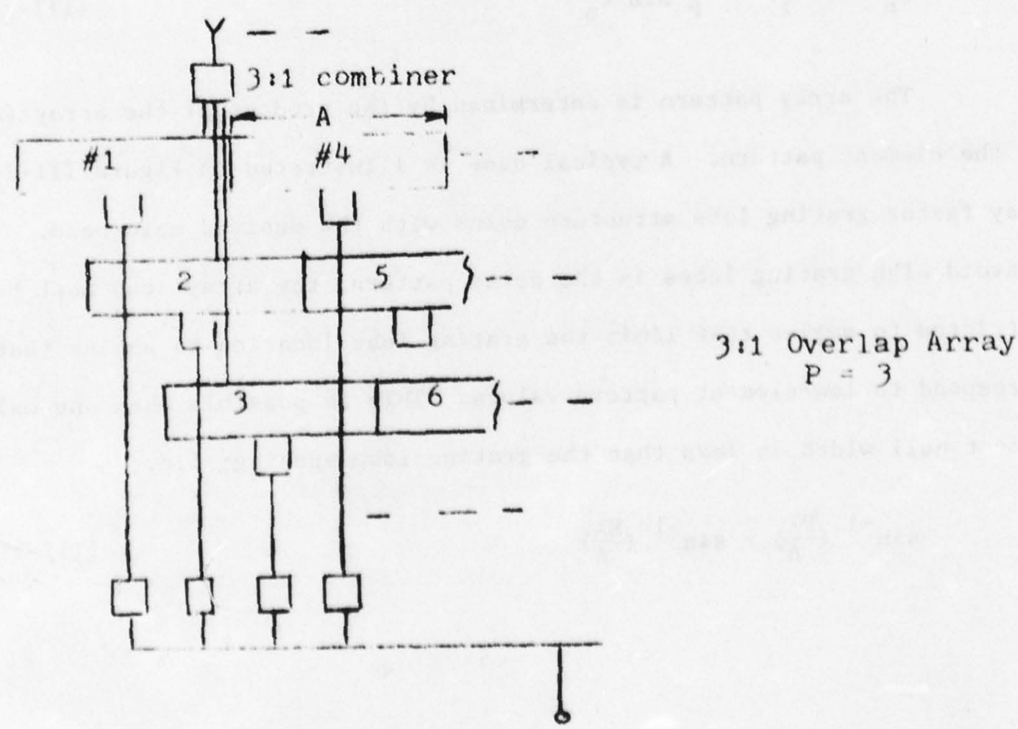

Fig. III.1 Overlapped Array Block Diagram

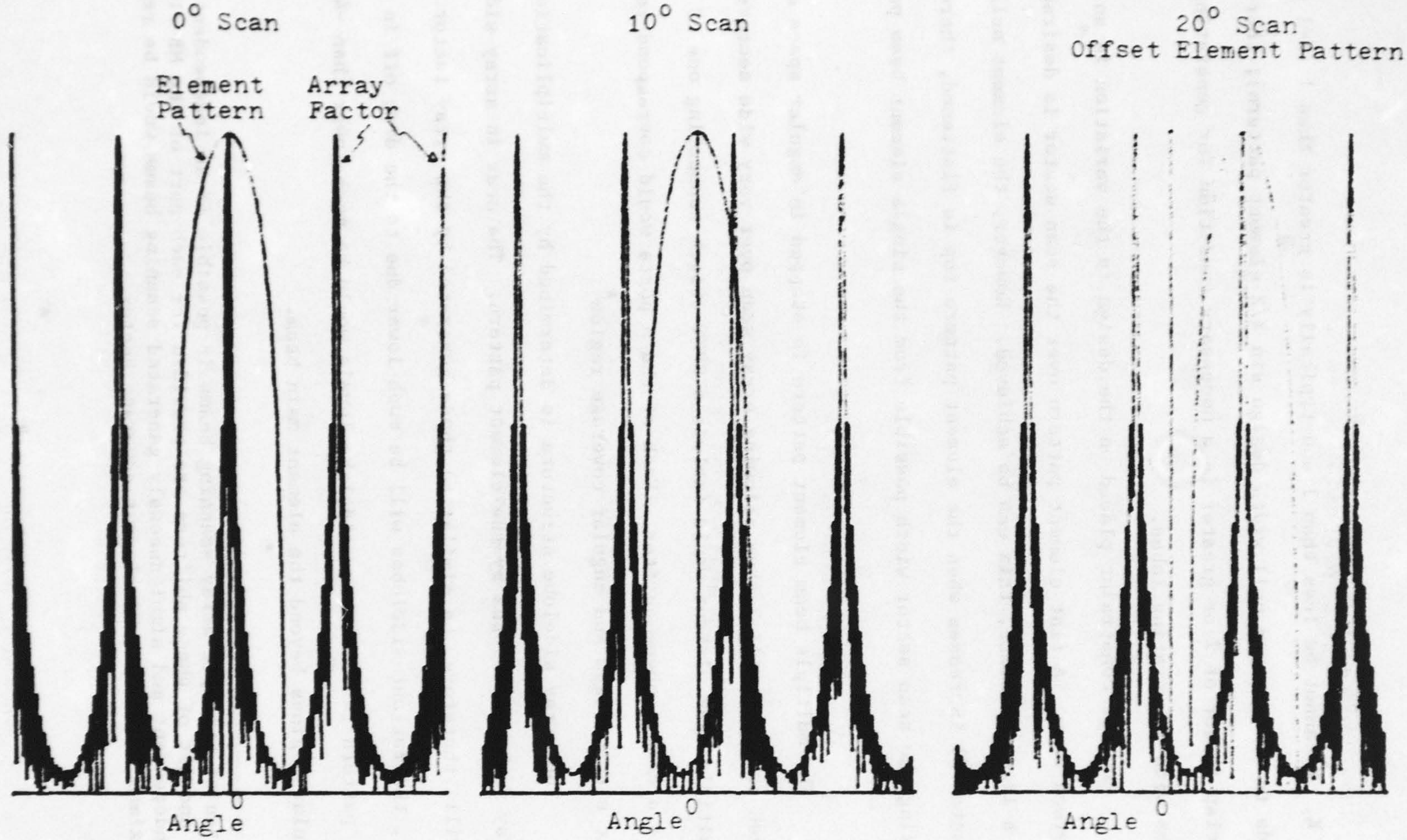

Fig. III.2 Array Pattern Generation

or $P > K$. K cannot be less than 1 and typically is greater than 1 (K=1 corresponds to the minimum null width design sin X/X element pattern); therefore, an overlap factor of 2 or greater is a necessary condition for generating scan patterns with low-grating lobes.

Another constraint placed on the design is the variation in antenna gain versus scan. A flat element pattern over the scan sector is desirable; and to a limited extent, this can be achieved. However, the element null width (and factor K) increases when the element pattern top is flattened, thereby decreasing the scan sector width possible from the single element beam position.

The multiple beam element pattern is stepped in angular space as indicated in Figure III-2 thus allowing array scan over very wide sectors. Each multiple beam element would include a SPMT switch connecting one of "M" ports to a common phase shifter. Each of the M ports would correspond to a specific element beam and angular coverage region*.

The array sidelobe structure is determined by the multiplication of the array factor sidelobes by the element pattern. The near in array sidelobes will, therefore, be similar to those generated by the array factor. However, the far-out sidelobes will be much lower due to the drop off in element pattern level. These sidelobe levels would be much lower than -40 dB for angular regions beyond the element main beam.

---

*Formation of multiple-array scanning beams is possible if an independent power divider and set of phase shifters are provided for each port of the MB element. These independent and simultaneously generated scanning beams would be restricted to a maximum of one per MB element coverage sector.

B. Array Gain

Array gain and antenna efficiencies is computed by using the principle of superposition. The array geometry assumed is illustrated in Figure III-1 for a 2:1 and 3:1 element overlap design. The general P:1 overlap design is considered in deriving the gain expressions, while subsequent detail analysis will emphasize the P=2 case.

The P:1 combiner can take a number of forms depending upon the transmission line medium selected, frequency, bandwidth requirements, etc. A sample schematic for 2, 3, and 4:1 combiners are illustrated in Figure III-3. In general, the combiner will illustrate a power loss factor of P plus some I^2R insertion loss. Ignoring the insertion loss, each MB element will radiate a field, E_n:

$$E_n(\theta,\phi) = \left(\frac{1}{P}\right)^{1/2} A_n G_e^{1/2}(\theta,\phi) \qquad \text{(III-3)}$$

where: P = element overlap factor

A_n = element weight (voltage)

G_e = element pattern gain.

The array pattern is:

$$E(\theta,\phi) = \sum^{N} E_n \, e^{j(2\pi N \frac{A}{P} \sin\theta + \psi_n)} \qquad \text{(III-4)}$$

and the array gain at beam peak is:

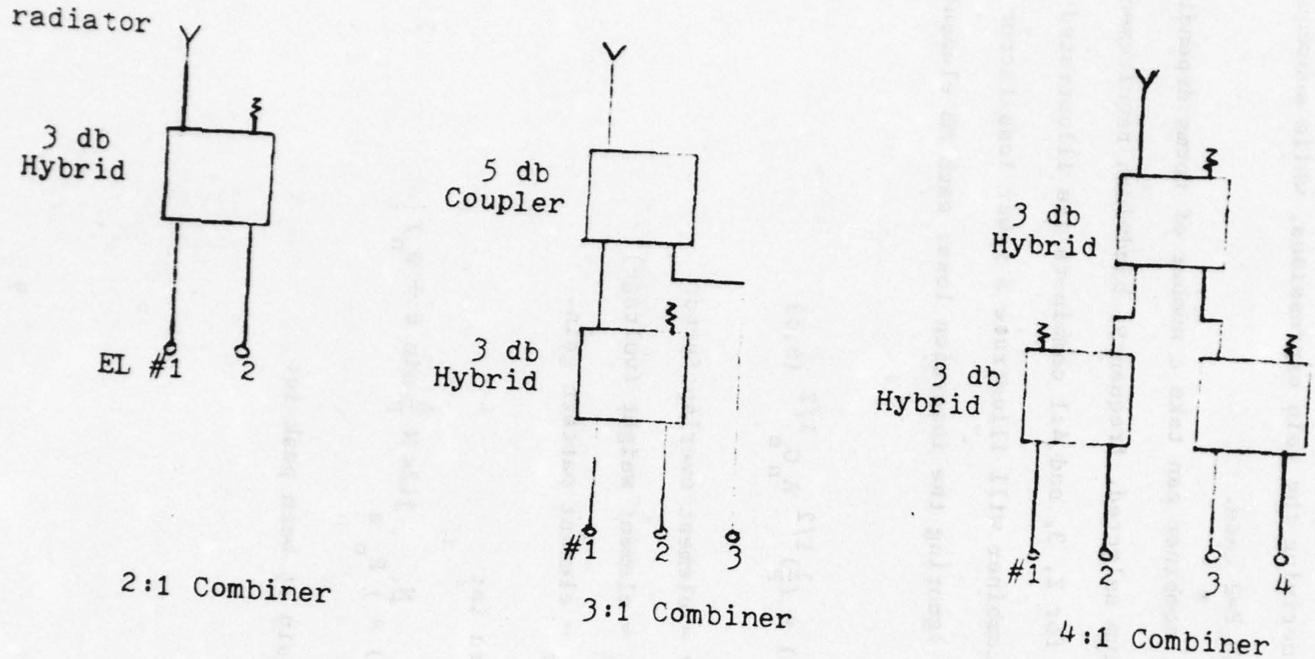

Fig. III.3 P:1 Combiners

$$G(\theta_o, \phi_o) = \frac{(\sum^{N} E_n)^2}{\sum^{N} A_n^2}$$

$$= \frac{G_e(\theta_o, \phi_o)}{P} \frac{(\sum^{N} A_n)^2}{\sum^{N} A_n^2} \quad . \qquad \text{(III-5)}$$

The array distribution pattern efficiency, is defined as

$$\varepsilon_a = \frac{1(\sum^{N} A_n)^2}{N \sum^{N} A_n^2} \qquad \text{(III-6)}$$

$\varepsilon_a = 1$ *for a uniformly illuminated array, i.e., a 100% efficient design;* $\varepsilon_a = 0.9$ for a 90% efficient design, etc.

Element gain is defined as

$$G_e(\theta_o, \phi_o) = \frac{2A}{\lambda} \varepsilon_e \qquad \text{(III-7)}$$

where ε_e = element pattern efficiency and the total array length is

$$L = \frac{N+P-1}{P} A \qquad \text{(III-8)}$$

Substituting (6), (7), and (8) into (5), we get

$$G(\theta_o, \phi_o) = \frac{N}{N+P-1} \varepsilon_e \varepsilon_a \frac{2L}{\lambda} \quad . \qquad \text{(III-9)}$$

Since the maximum gain, G_o, from an array of length L is $2L/\lambda$.

$$G(\theta_o, \phi_o) = \frac{N}{N+P-1} \varepsilon_e \varepsilon_a G_o \qquad \text{(III-10)}$$

$$= \text{L.F. } \varepsilon_e \varepsilon_a G_o \qquad \text{(III-11)}$$

where:

$$\text{Loss factor} = \text{L.F.} = \frac{N}{N+P-1} \qquad \text{(III-12)}$$

The principle effect on pattern gain in an overlapped array versus a standard non-overlapped array is the loss attributed to the overlap loss factor. This loss factor is plotted in Figures III-4 and III-5. In Figure III-4, the loss factor is plotted versus the number of array elements for overlap factors of 2 to 5. As indicated as the overlap factor increases, the loss also increases for a fixed number of array elements. However, as the overlap factor increases, the number of array elements must also increase if the element and array sizes are kept constant. This increase in number of elements counters to some extent the increase in loss factor due to larger P. Figure III-5 illustrates this fact. In this figure, the loss factor is plotted versus array aperture size normalized to the array element size. We see that the loss attributed to the overlap factor is less than 1 dB for all practical cases; i.e., the aperture of the full array is 4 or more times the element aperture. Furthermore, we see only small (tenths of a dB) increases in loss for P > 2.

Unity element and array factor efficiencies are achievable. This occurs for a uniform array excitation ($A_n = 1$ for all n) and a uniform element aperture distribution (such as obtained from a Butler Matrix). The net array gain at the element beam pointing angle would then be equal to $2L/\lambda$ less the loss factor. As the array is scanned away from the element beam peak, the array gain would decrease at the same rate as the element pattern.

The uniform array illumination results in the familiar sin X/X type array pattern which gets multiplied by the element pattern. Close-in sidelobes

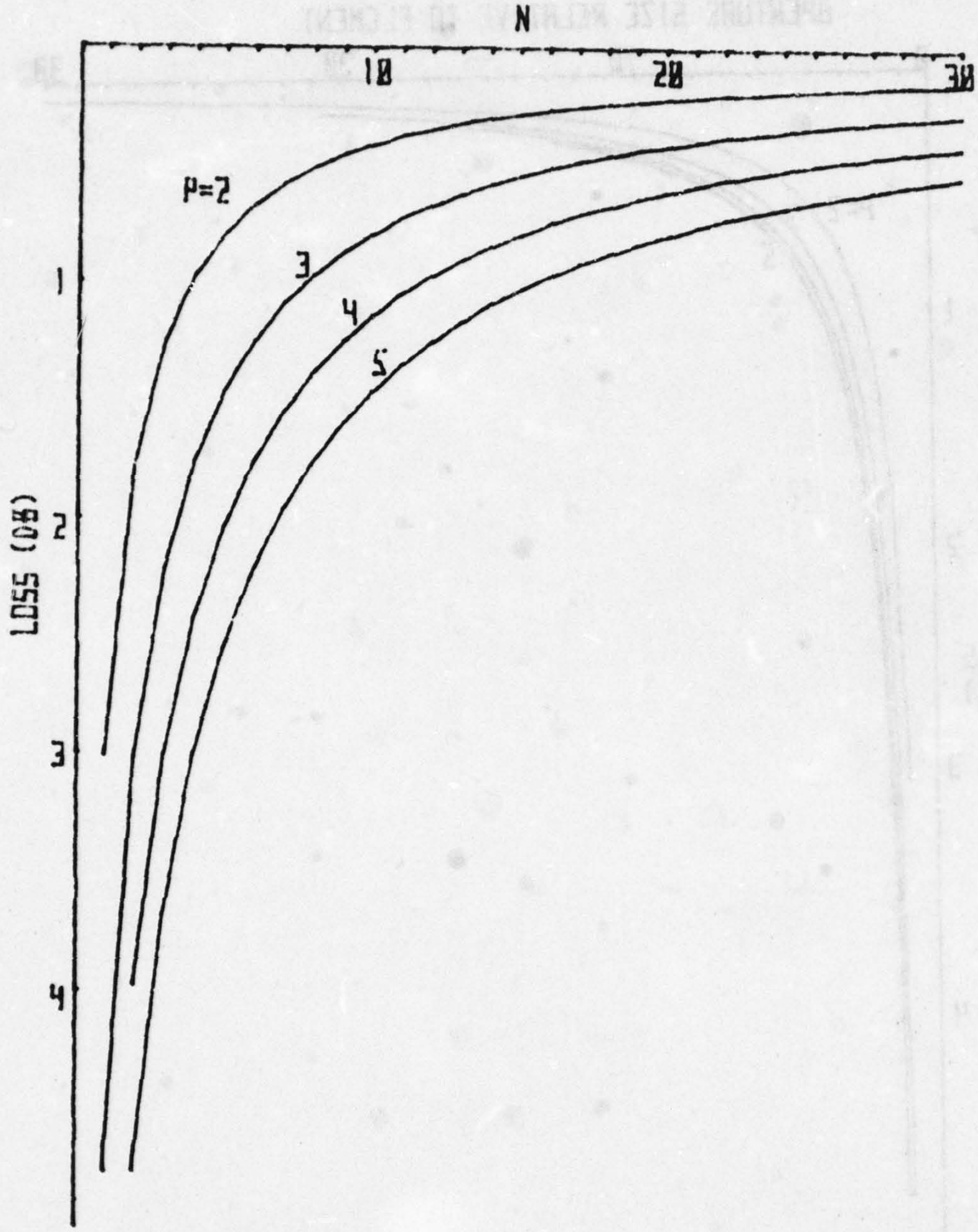

FIG. III.4 OVERLAP LOSS FACTOR VS. NUMBER OF ELEMENTS

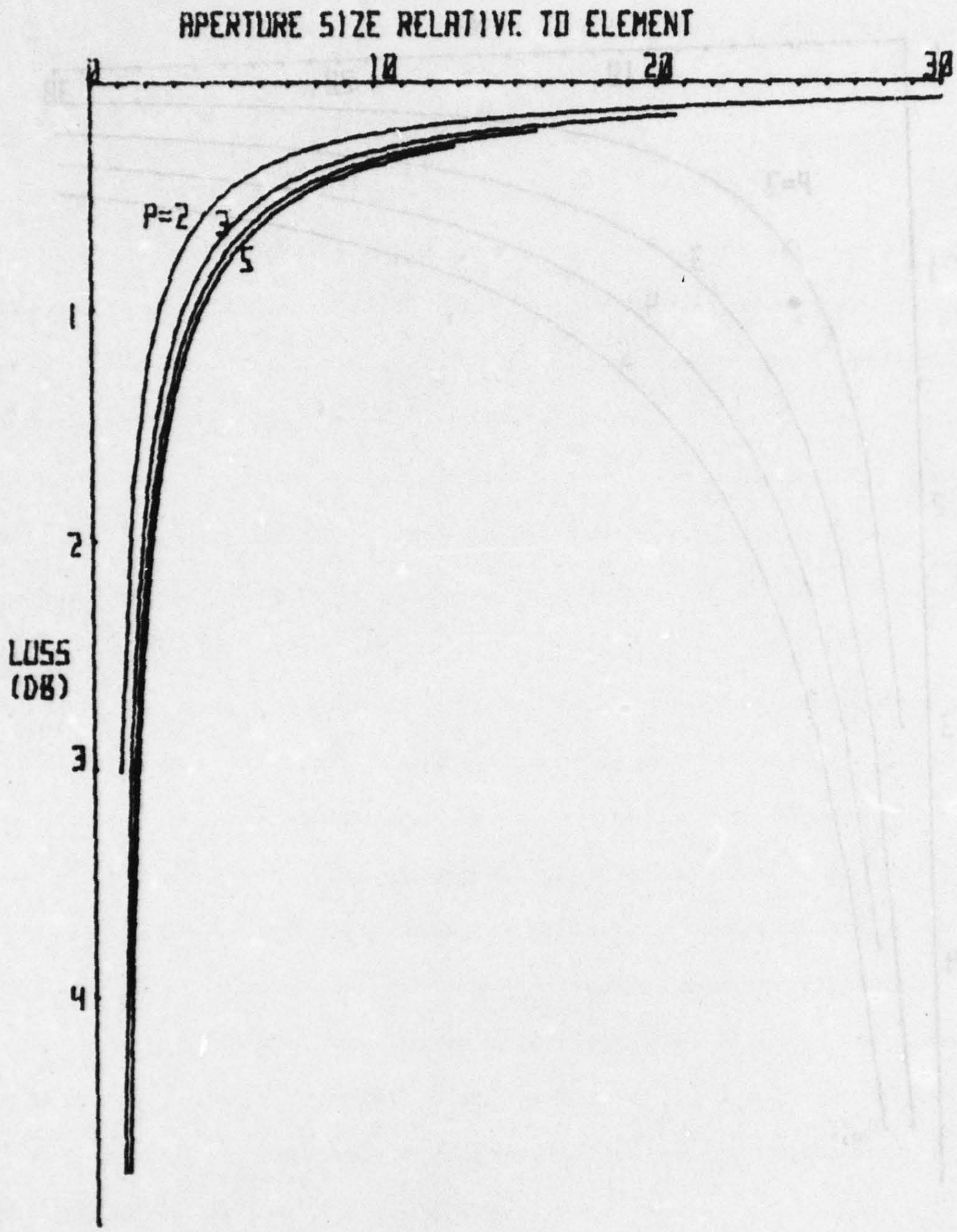

FIG. III.5 OVERLAP LOSS FACTOR VS. ARRAY APERTURE SIZE will be high, i.e., 13.3 dB and 17.8 dB first and second sidelobes with far-out sidelobes dropping more rapidly as the element pattern factor starts to dominate. Array factor efficiencies other than unity (tapored distribution) are, therefore, desirable if low close-in sidelobes are required. This is true for both overlapped and non-overlapped array designs and results in similar gain reductions for both approaches.

The element factor gain and efficiency is very much related to other system requirements including grating lobes level, scan sector size, gain variation versus scan, number of elements, and number of beams generated by the multiple-beam element. Further discussion of the trade offs associated with the element patterns achievable is presented in the following sections.

C. Element Patterns

The multiple-beam element design can utilize a multiple-beam lens feed or a matrix feed network. The choice of feed type depends on performance specifications and/or cost objectives of the system.

Both techniques have a variety of element pattern shape options. The Butler Matrix feed technique was chosen for close examination in this study. This matrix feed type was chosen as a candidate component in the overlapped array concept because of its low loss characteristics, simplicity, and established capabilities, while providing suitable characteristics for a class of applications. Other matrix and lens feed systems provide a wider choice of design options and are clearly possible, and in some high performance systems may be preferable. The analysis presented in this report demonstrates the capabilities of the overlapped array with the Butler Matrix feed and points out the performance limitations that are peculiar to the Butler feed.

The Butler Matrix generates a uniform amplitude and linear phase distribution to 2^Q ports when any one of the 2^Q input beam ports is energized. This distribution generates a sin X/X beam pattern at an angle separated from the adjacent beam by λ/A in $\sin\theta$ space, where A, the element aperture, is equal to $d\cdot 2^Q$. This is illustrated in Figure III-7 for the 8 port Butler Matrix (Q=3) schematically shown in Figure III-6. The pattern illustrated assumes the matrix output ports are directly feeding elementary radiators spaced $\lambda/2$ apart. Each radiator is assumed to have a $\cos\theta$ gain factor. The patterns peak at $\pm \sin^{-1}\left(\frac{2B-1}{2}\frac{\lambda}{A}\right)$ where B is the beam port number, and cross at the -4 dB level. Wider spaced radiators result in a larger effective aperture and a sin X/X pattern that starts to display grating lobes for the higher numbered beams. This is illustrated in Figure III-8 for a 0.8λ radiator spacing.

The single beam port patterns can be combined in a number of ways to generate broader patterns, flat top patterns, and low sidelobe patterns. Examples of in-phase and quadrature phase combining of adjacent beams are shown in Figure III-9. The quadrature-phased beams result in a flattening of the beam top, but at the expense of a relatively high sidelobe (approximately -11 dB). The in-phase case results in a cosine aperture distribution with a pattern exhibiting a single peaked beam with a -23 dB first sidelobe*. In both cases, the main beam null width is $\sin^{-1}\left(\frac{3\lambda}{A}\right)$, i.e., the "K" value defined in Figure III-2 is 1.5, and, therefore, satisfies the requirement that P > K for overlap factors of 2:1 or greater.

---

* The -23 dB first sidelobe applies to large apertures such as those formed from 8 port Butler matrices or larger.

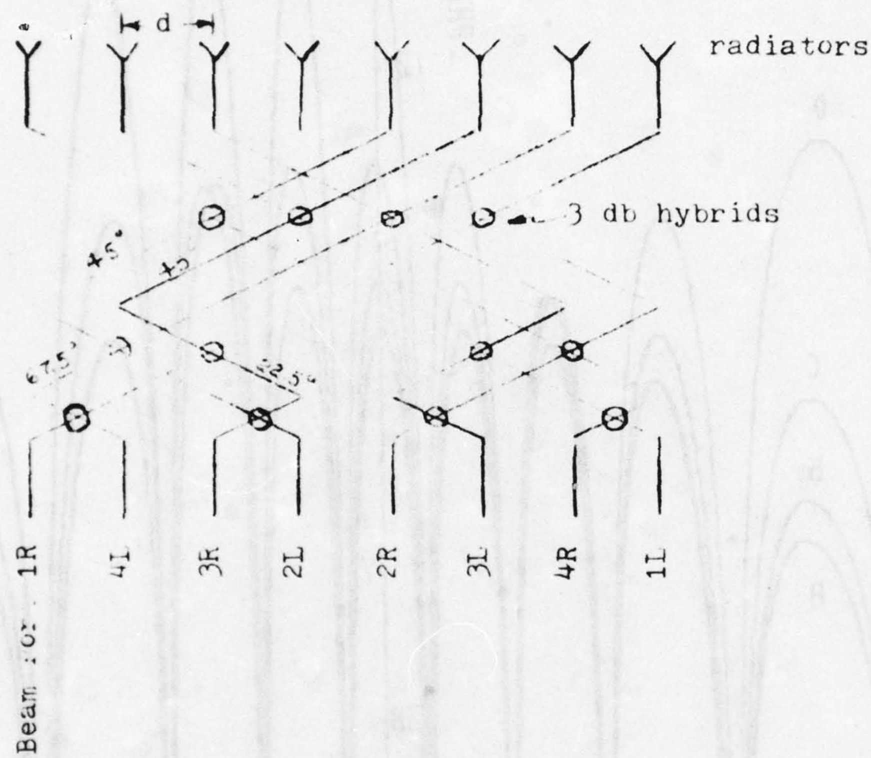

Fig. III.6 8 Port Butler Matrix Schematic

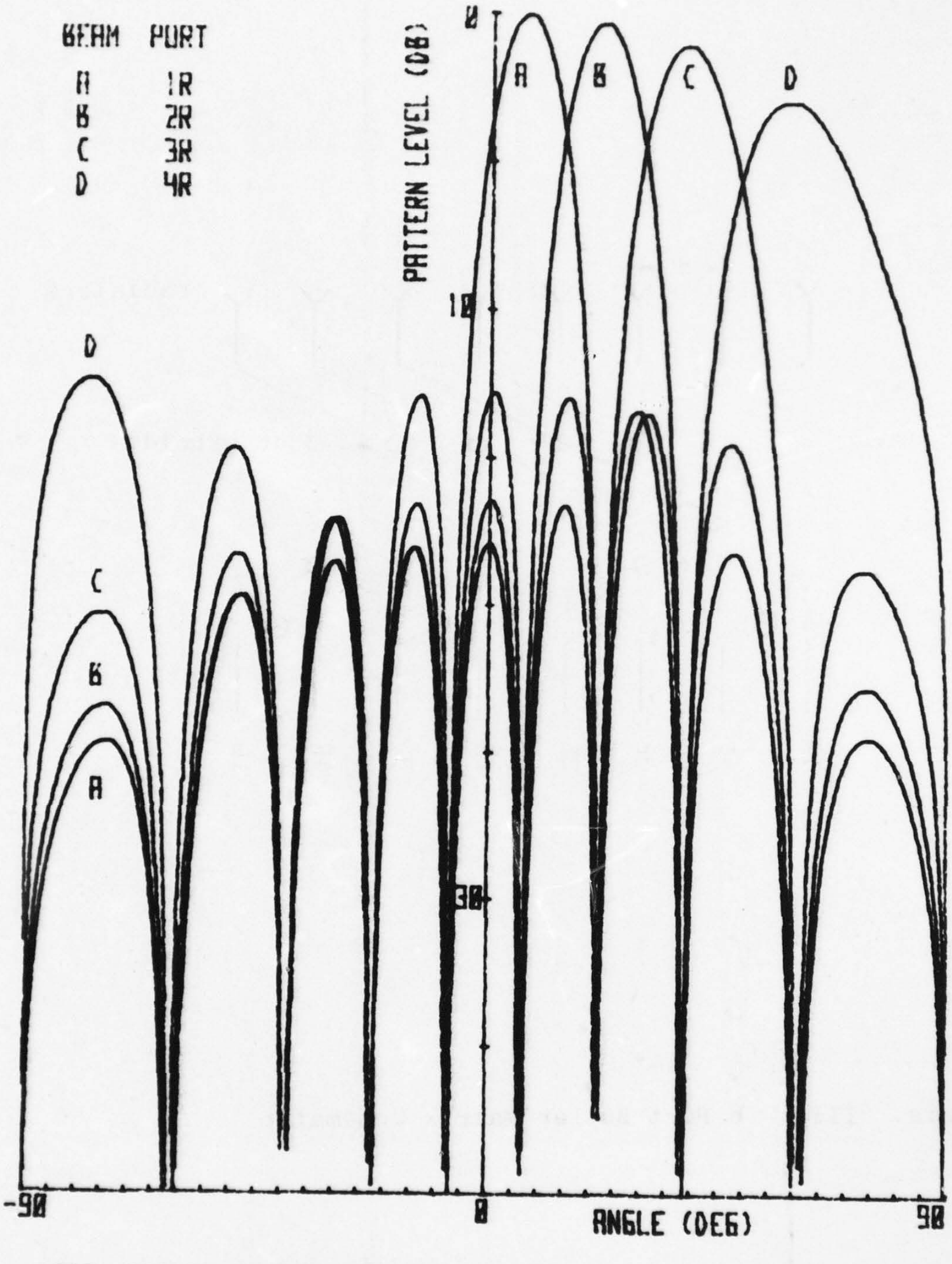

FIG. III.7 SINGLE PORT BUTLER MATRIX - .5λ RADIATOR SPACING

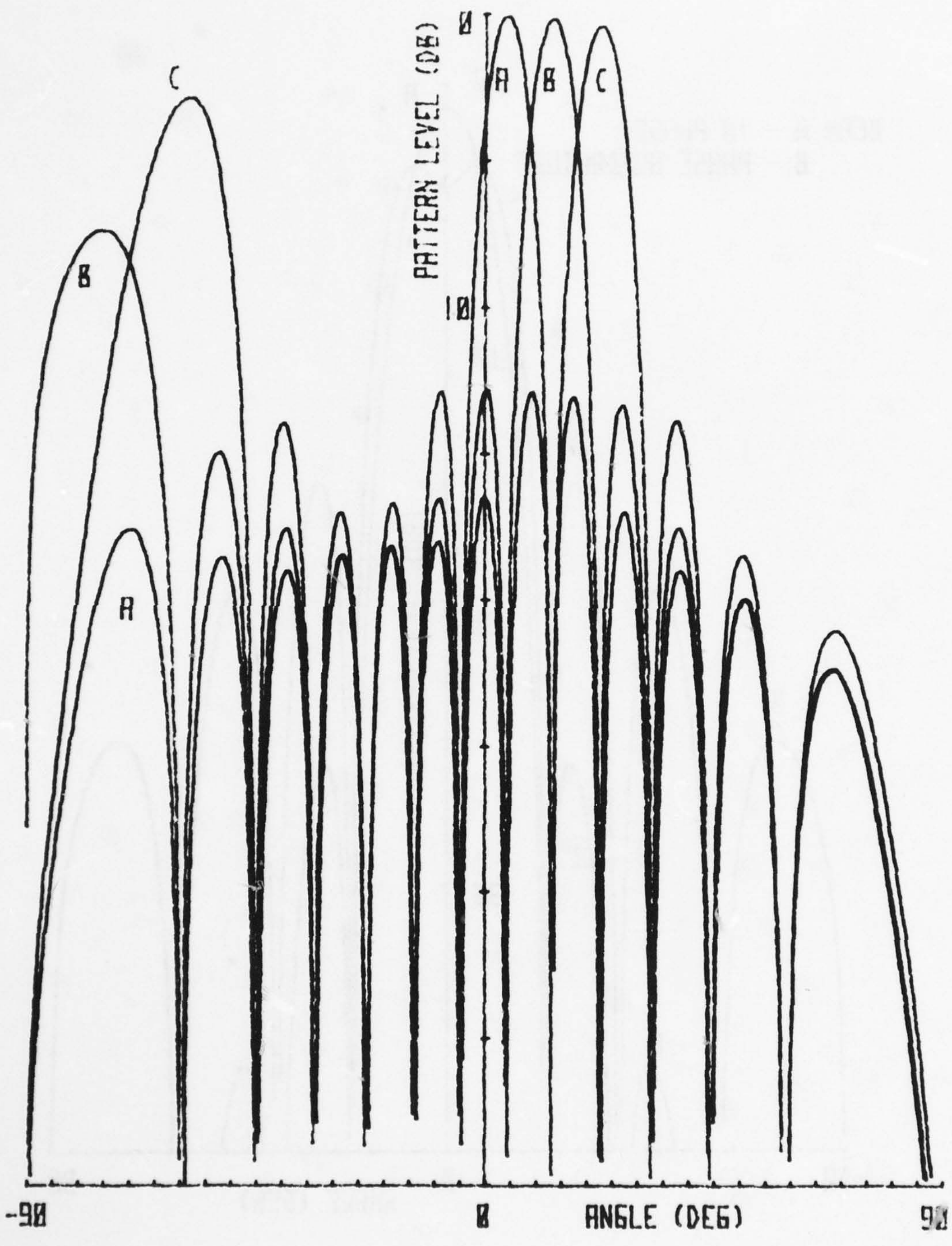

FIG. III.8 SINGLE PORT BUTLER MATRIX PATTERN- .8λ RADIATOR SPACING

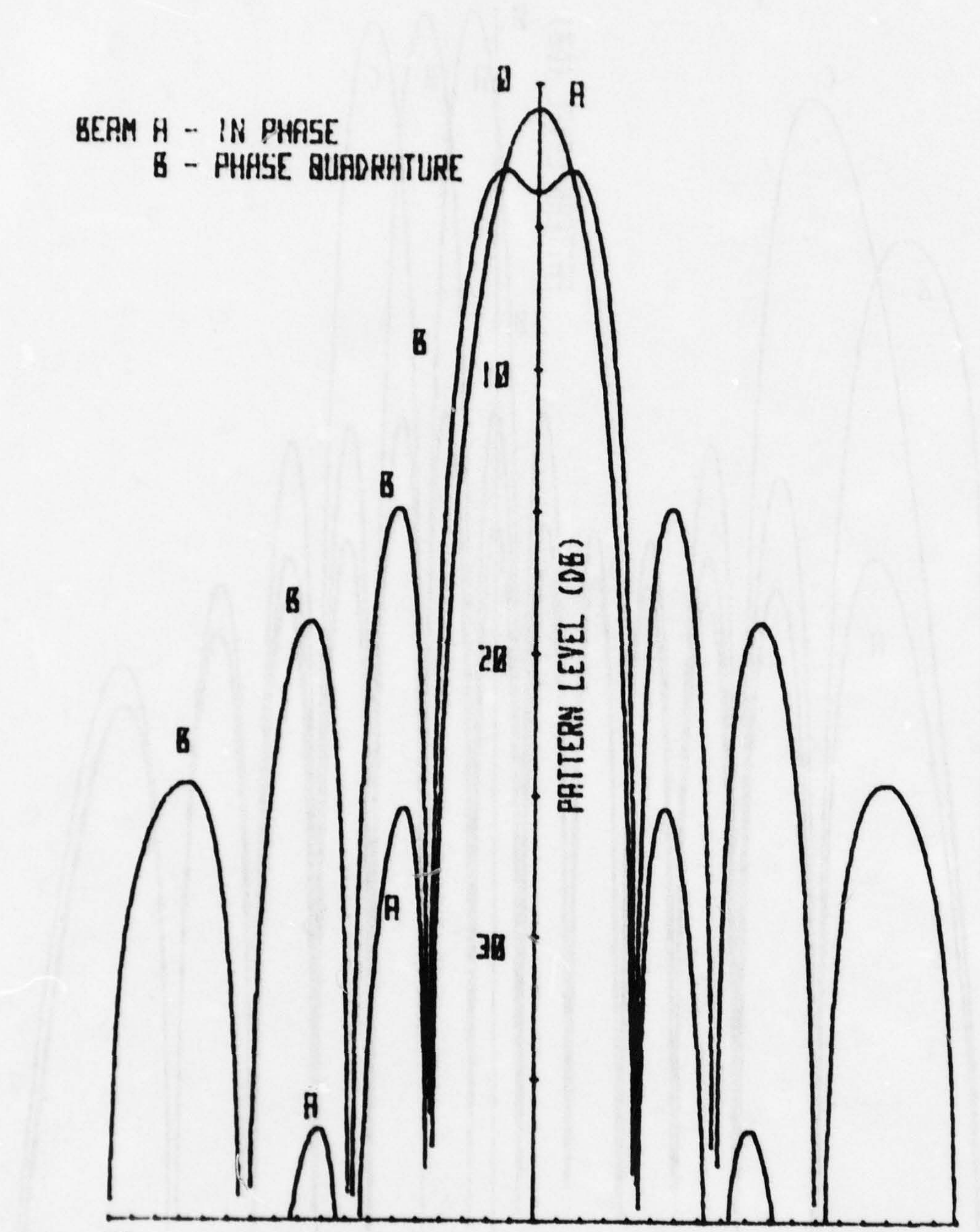

FIG. III.9 2 PORT BUTLER MATRIX PATTERNS

Combining three adjacent beams for a flat top pattern is illustrated in Figure III-10. The null width widens with a resultant value of 2 for K. This pattern is, therefore, most useful for overlap factors of 3:1 or greater and is borderline for a 2:1 overlap factor. Combining greater numbers of beams results in further widening of the pattern and the requirement for greater overlap factors.

The above idealized patterns are modified in actual practice due to amplitude and phase errors generated by the less-than-perfect manufacturing process of the matrix. Feed system performance published on data sheets for Butler matrices* indicate antenna port amplitude and phase errors of 0.5 dB rms and 3° rms, respectively. Element patterns were computed assuming these errors across the aperture for the 2 port inphase element (cosine aperture illumination). An independent, uniform error distribution was assumed for each beam before summation. Ten such cases, each with independent sets of errors, are shown plotted in Figure III-11. The average element voltage pattern is illustrated in Figure III-12, where the average pattern was computed from equation

$$E_a = \frac{1}{N} \sum^{N} E_n \quad . \tag{III-13}$$

This average pattern when multiplied by the array factor can be used to estimate the array pattern. It is particularly informative in calculating beam peak and grating lobe levels. These conditions occur when all the elements are in-phase, or:

---

*Sanders Associates, Inc., TA-500 Series

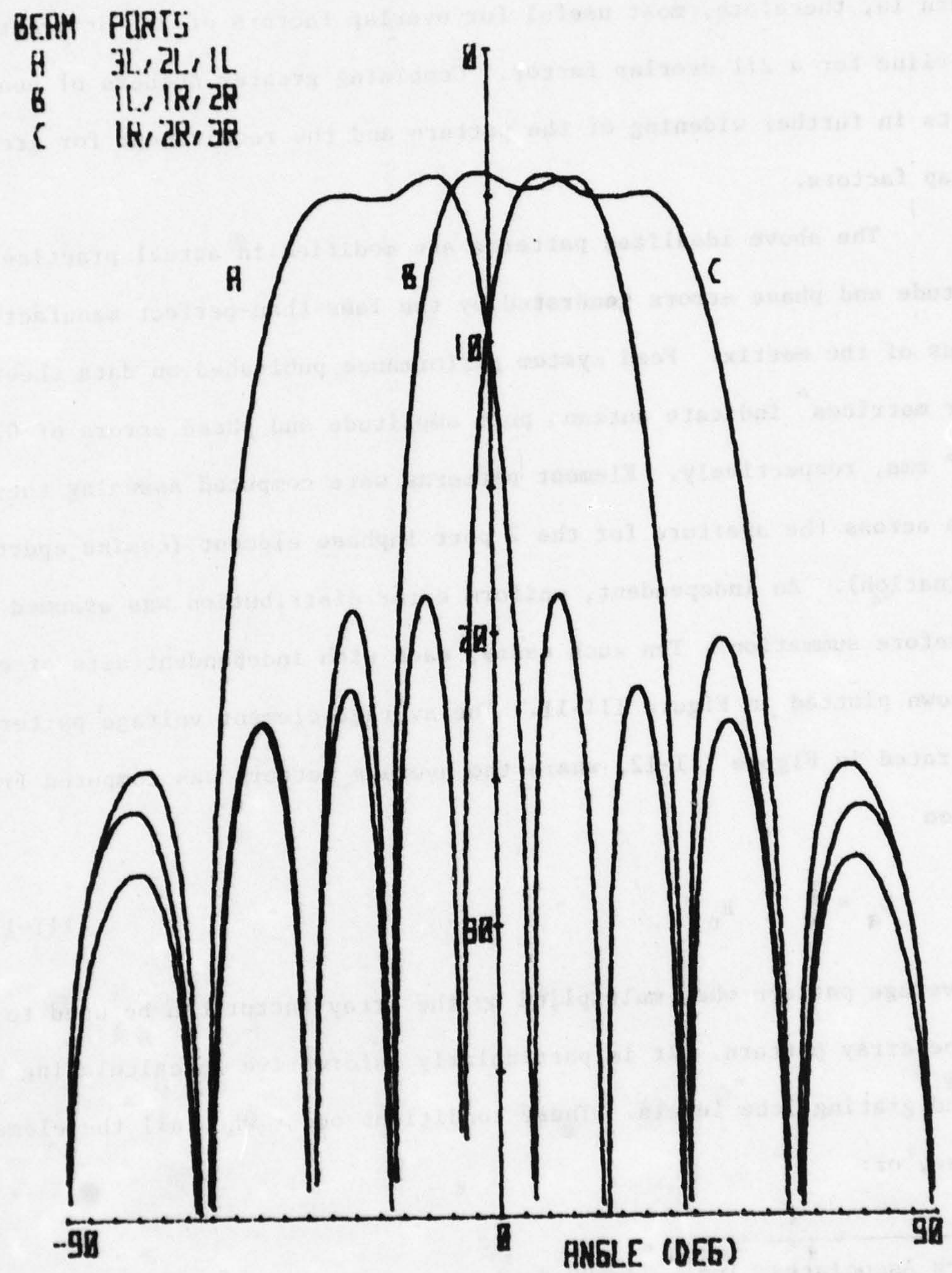

FIG. III.10 3 PORT BUTLER MATRIX PATTERNS

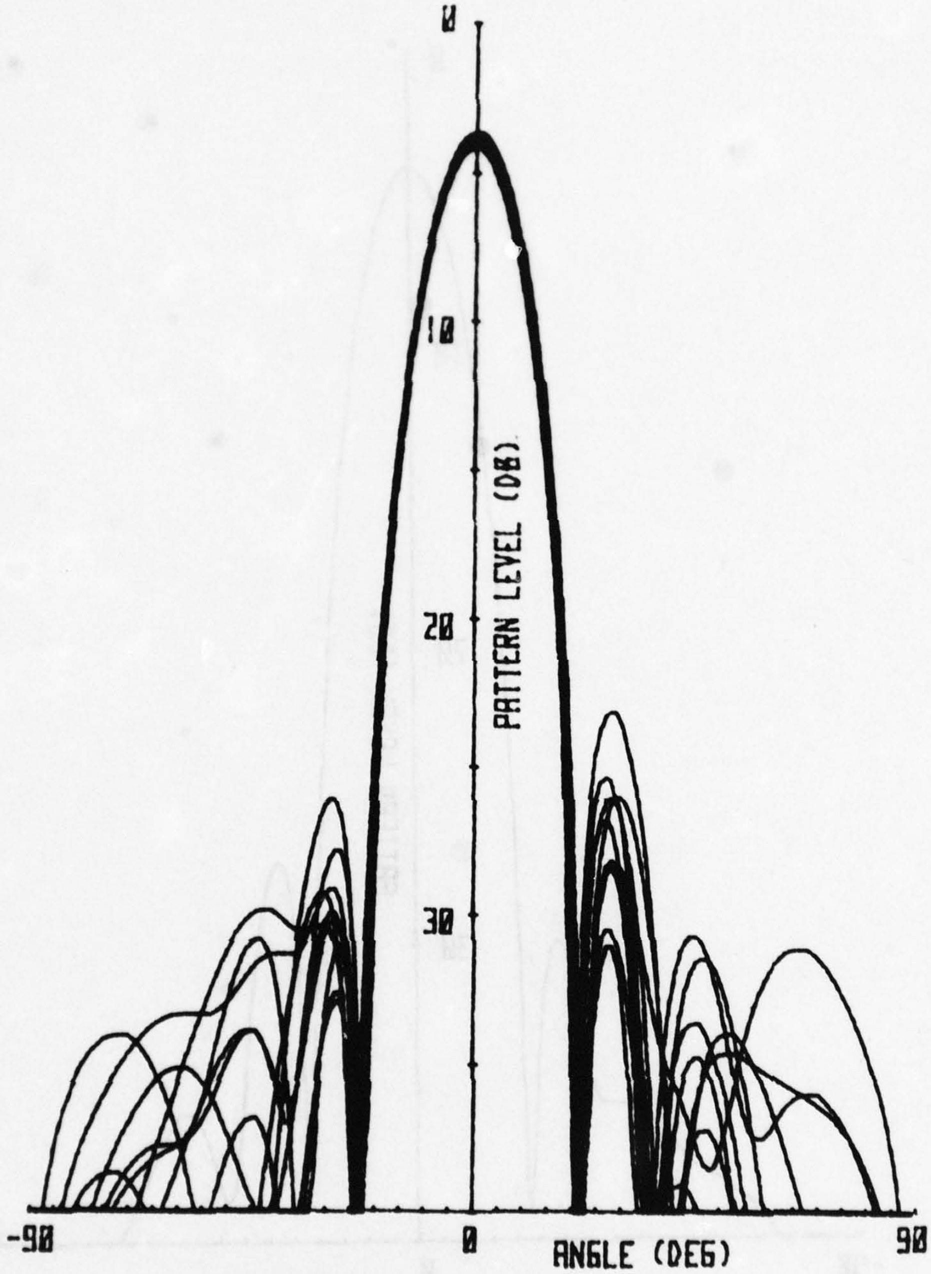

FIG. III.11 ERROR AFFECTS ON ELEMENT PATTERNS

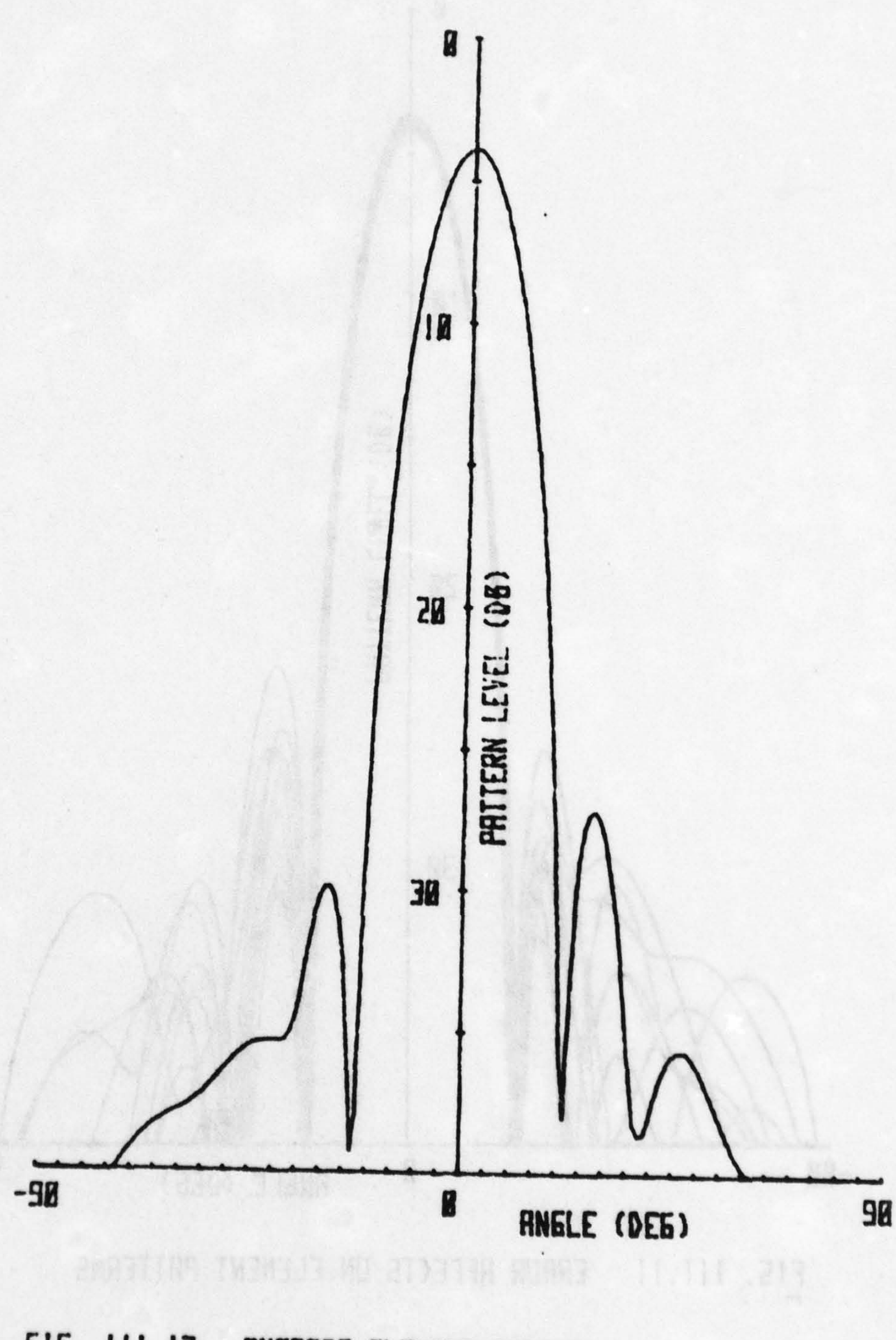

FIG. III.12 AVERAGE ELEMENT PATTERN

$$E_{peak} = \sum^{N} A_n \, E_n(\theta_p) \qquad \text{(III-14)}$$

$$E_{q.L.} = \sum A_n \, E_n(\theta_{g.L.}) \qquad \text{(III-15)}$$

In the case of the uniformally illuminated array A_n=1 for all n, and

$$E_{peak} = N \, E_a(\theta_p) \qquad \text{(III-16)}$$

$$E_{q.L.} = N \, E_a(\theta_{g.L.}) \qquad \text{(III-17)}$$

The above element designs are generated from lossless networks. Resistive taporing of the element aperture can be used to further tailor the element pattern at the expense of some I^2R losses. This provides additional pattern options for broadening of the element beam and specifying its sidelobes without affecting the beam location. This is of particular interest when considering scan patterns, as is discussed in the next section.

An aperture tapor of interest is the Tchebyscheff distribution. I^2R and directivity loss versus sidelobe level for a single port Tchebyscheff beam is shown in Figure III-13. For comparison, the directivity loss (relative to a uniform aperture distribution) for the in-phase 2 port design (no resistive tapor) is .9 dB and generates a -23 dB first sidelobe and -30 dB second sidelobe. The "K" factor for the Tchebyscheff and untapored 1, 2, and 3 port beams is shown in Figure III-14.

The interesting feature of the Tchebyscheff-element pattern is the uniformity of the sidelobe levels. When combining two of these beams, if the beam separation is proper, very near perfect cancellation of the sidelobes can

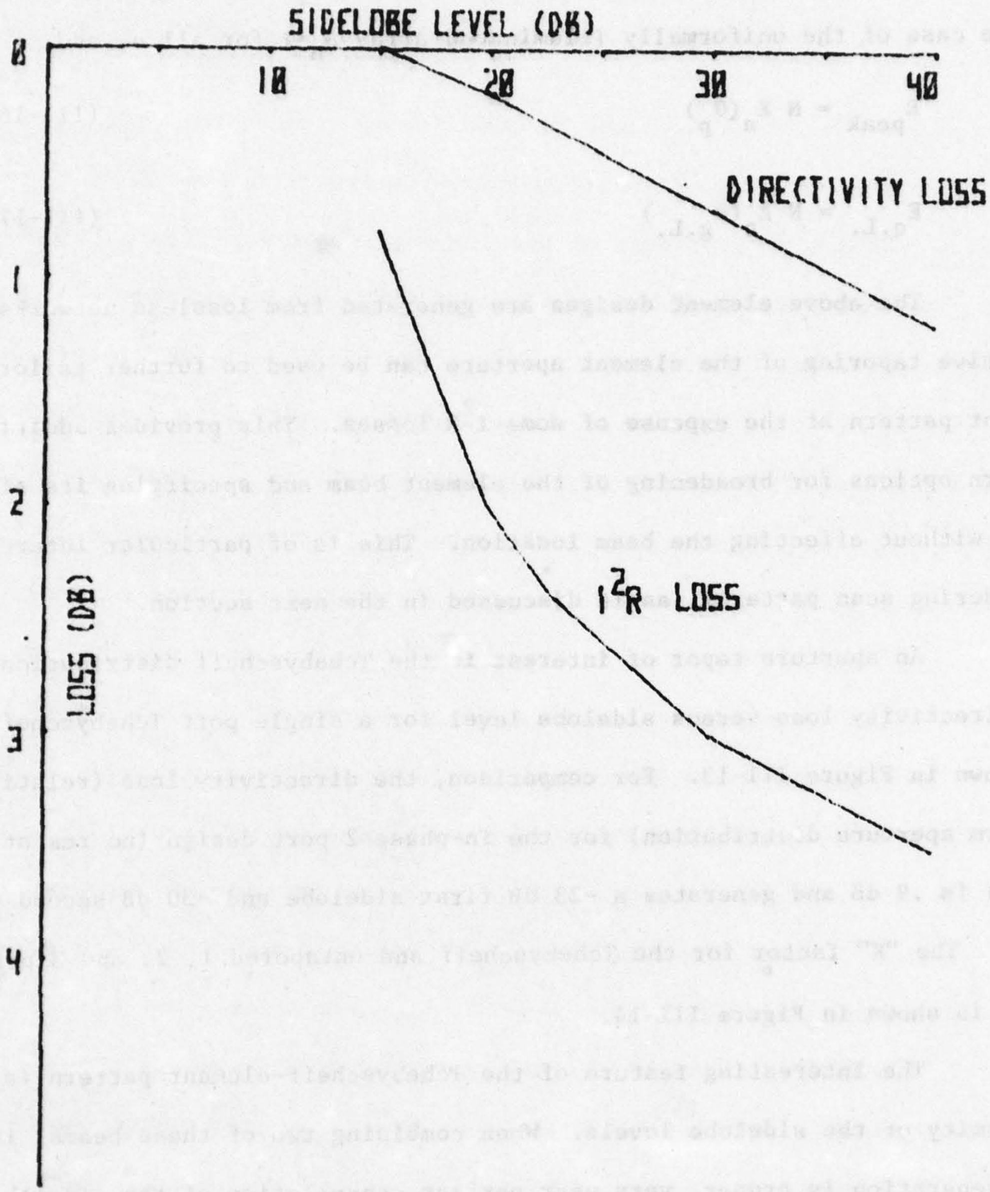

FIG. III.13 TCHEBYSCHEFF TAPOR LOSSES

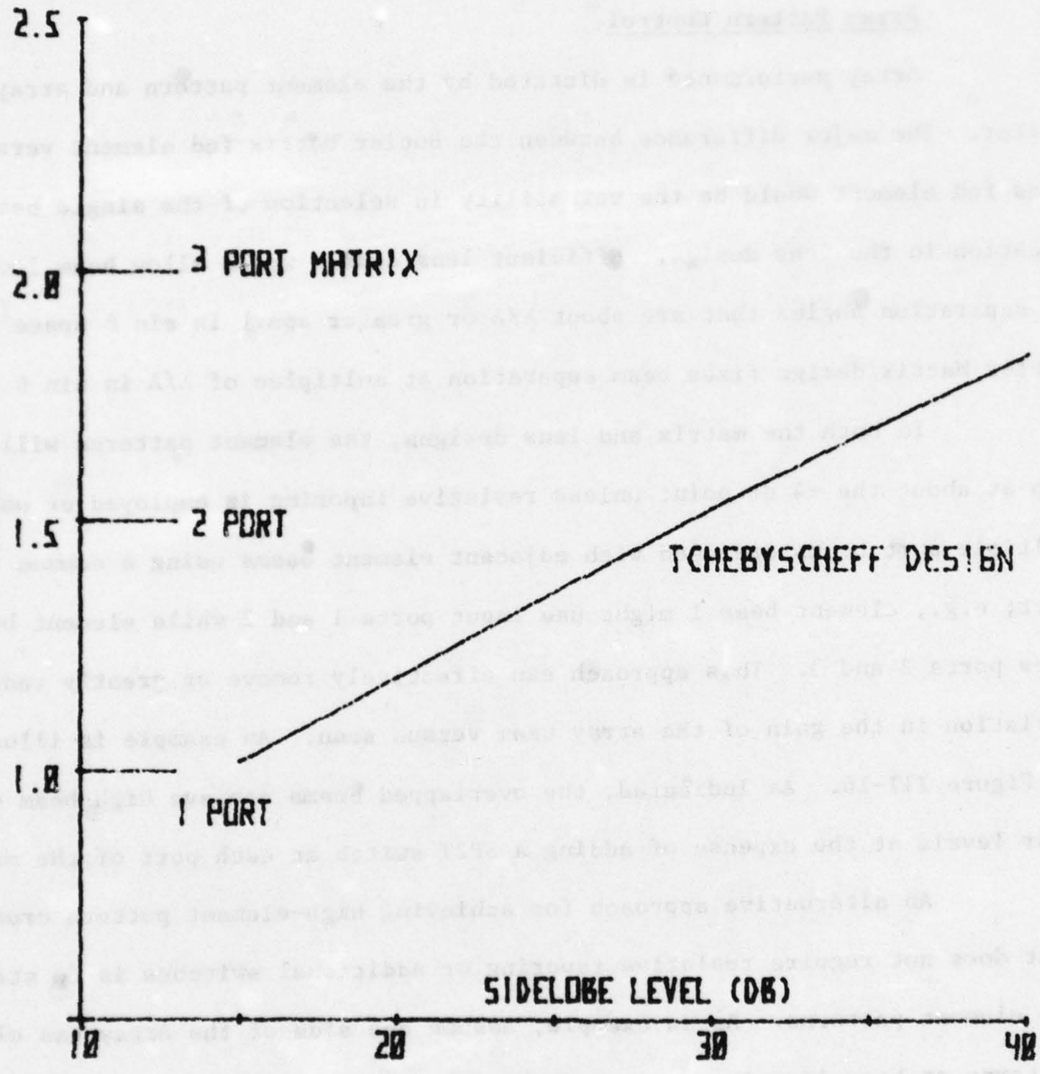

FIG. III.14 K FACTOR

occur. This is illustrated in Figure III-15 for an in-phase 2 port Butler Matrix beam that has resistive taporing of the aperture equivalent to a 15 dB and 20 dB Tchebyscheff design.

D. Array Pattern Control

Array performance is dictated by the element pattern and array factor. The major difference between the Butler Matrix fed element versus the lens fed element would be the versatility in selection of the single beam port location in the lens design. Efficient lens design would allow beam locations at separation angles that are about λ/A or greater apart in $\sin\theta$ space[1]. The Butler Matrix design fixes beam separation at multiples of λ/A in $\sin\theta$ space.

In both the matrix and lens designs, the element patterns will overlap at about the -4 dB point unless resistive taporing is employed or unless multiple port beams are used with adjacent element beams using a common input port; e.g., element beam 1 might use input ports 1 and 2 while element beam 2 uses ports 2 and 3. This approach can effectively remove or greatly reduce variation in the gain of the array beam versus scan. An example is illustrated in Figure III-16. As indicated, the overlapped beams achieve high-beam crossover levels at the expense of adding a SP2T switch at each port of the matrix.

An alternative approach for achieving high-element pattern cross over that does not require resistive taporing or additional switches is to stagger the element patterns. As an example, assume one side of the array has element patterns at beam locations generated by in-phase addition of ports 4L&3L, 2L&1L, 1R&2R, 3R&4R. The other side would have beams determined by ports 3L&2L, 1L&1R, 2R&3R (see Figure III-17). The "average" element pattern for the

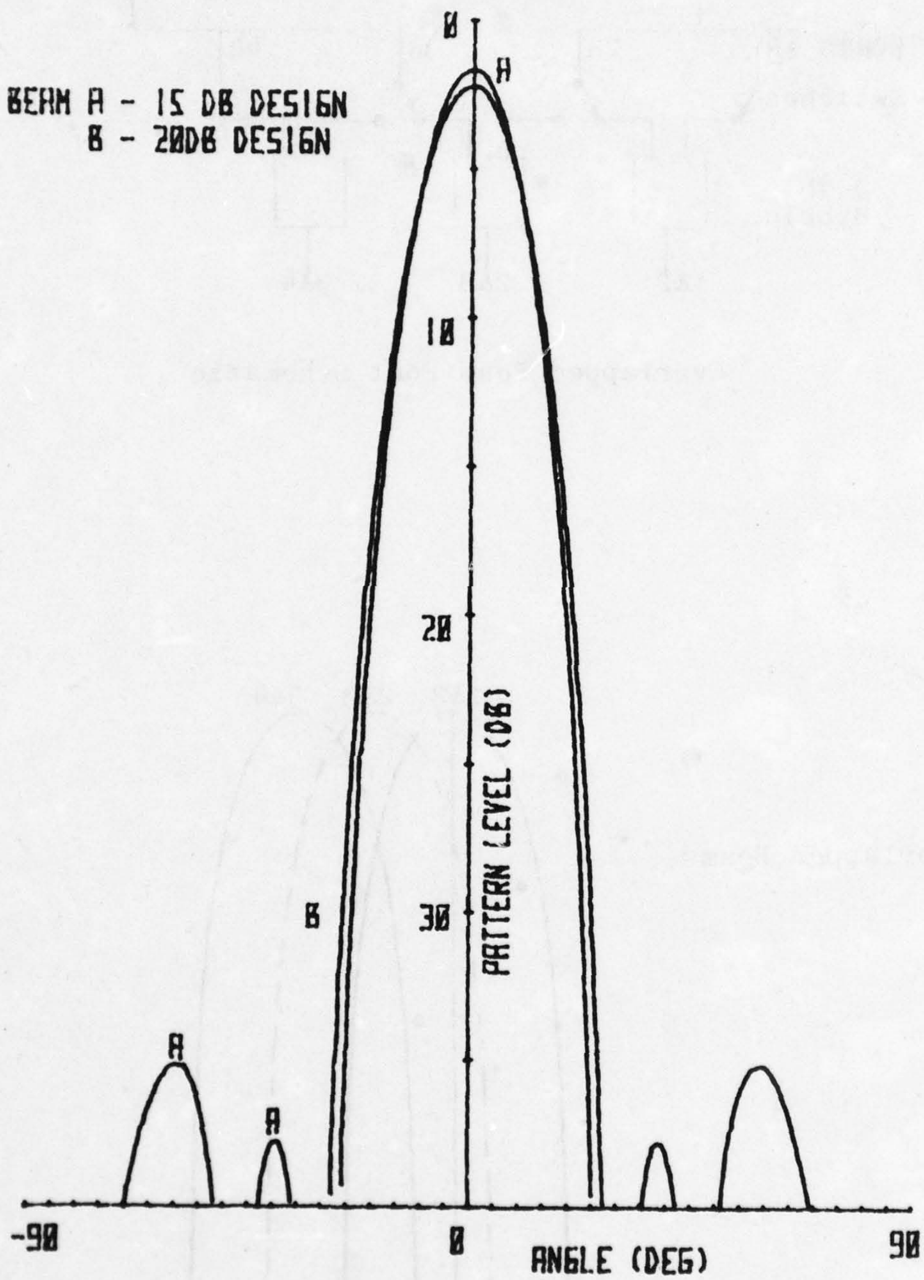

FIG. III.15 2 PORT BUTLER MATRIX PATTERN WITH TCHEBYSCHEFF WEIGHTING

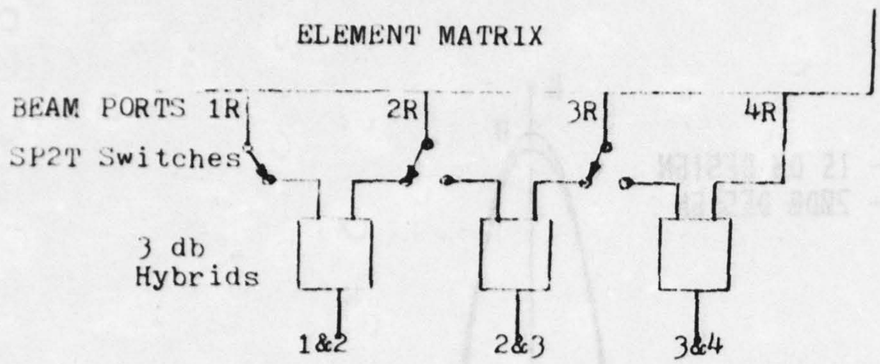

Overlapped Beam Port Schematic

Overlapped Beams

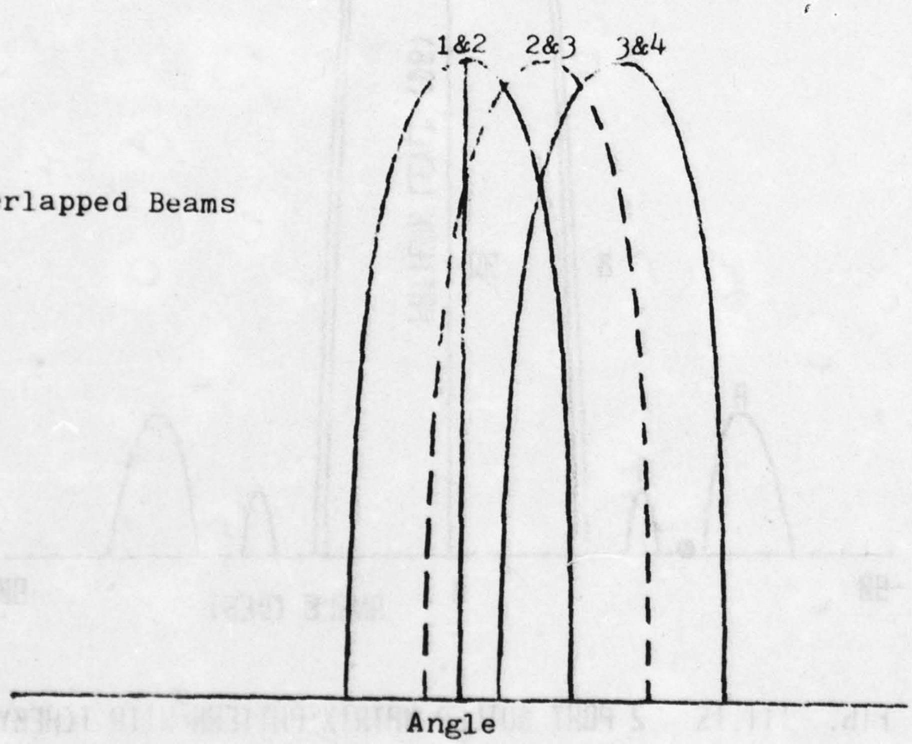

Fig. III.16 Overlapped Element Patterns

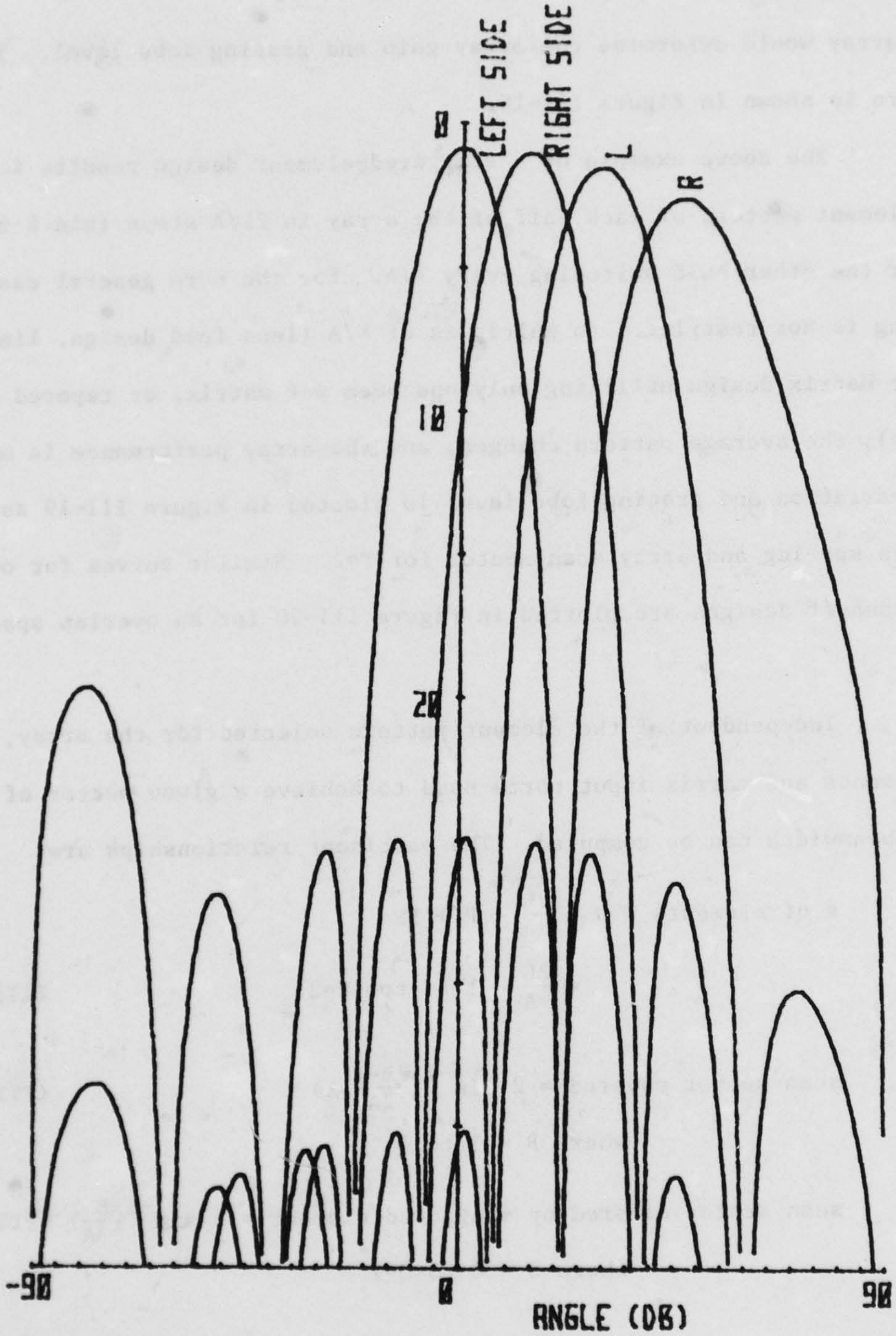

FIG. III.17 STAGGERED 2 PORT PATTERNS

full array would determine the array gain and grating lobe level. This average pattern is shown in Figure III-18.

The above example of a staggered-element design results in stepping the element pattern of each half of the array in $2\lambda/A$ steps ($\sin\theta$ space) with one or the other half switching every λ/A. For the more general case where the spacing is not restricted to multiples of λ/A (lens feed design, limited scan Butler Matrix design utilizing only one beam per matrix, or tapored aperture design), the average pattern changes, and the array performance is modified. Gain variation and grating lobe level is plotted in Figure III-19 as a function of this spacing and array scan sector for P=2. Similar curves for overlapped Tchebyscheff designs are plotted in Figure III-20 for an overlap spacing of λ/A.

Independent of the element pattern selected for the array, the number of elements and matrix input ports used to achieve a given sector of scan and array beamwidth can be computed. The pertinent relationships are:

$$\# \text{ of elements} = N = \frac{PL}{A} - P + 1$$

$$= \frac{2L}{A} - 1 \quad \text{for } P=2 \qquad \text{(III-18)}$$

$$\text{scan sector covered} = 2 \sin^{-1}\left(\frac{2B-1}{2A}\lambda\right) \qquad \text{(III-19)}$$

where B = 1 to Q

$$\text{scan sector covered by staggered element} = 2 \sin^{-1}\left(\frac{B}{A}\right) \qquad \text{(III-20)}$$

where B = 0 to Q-1

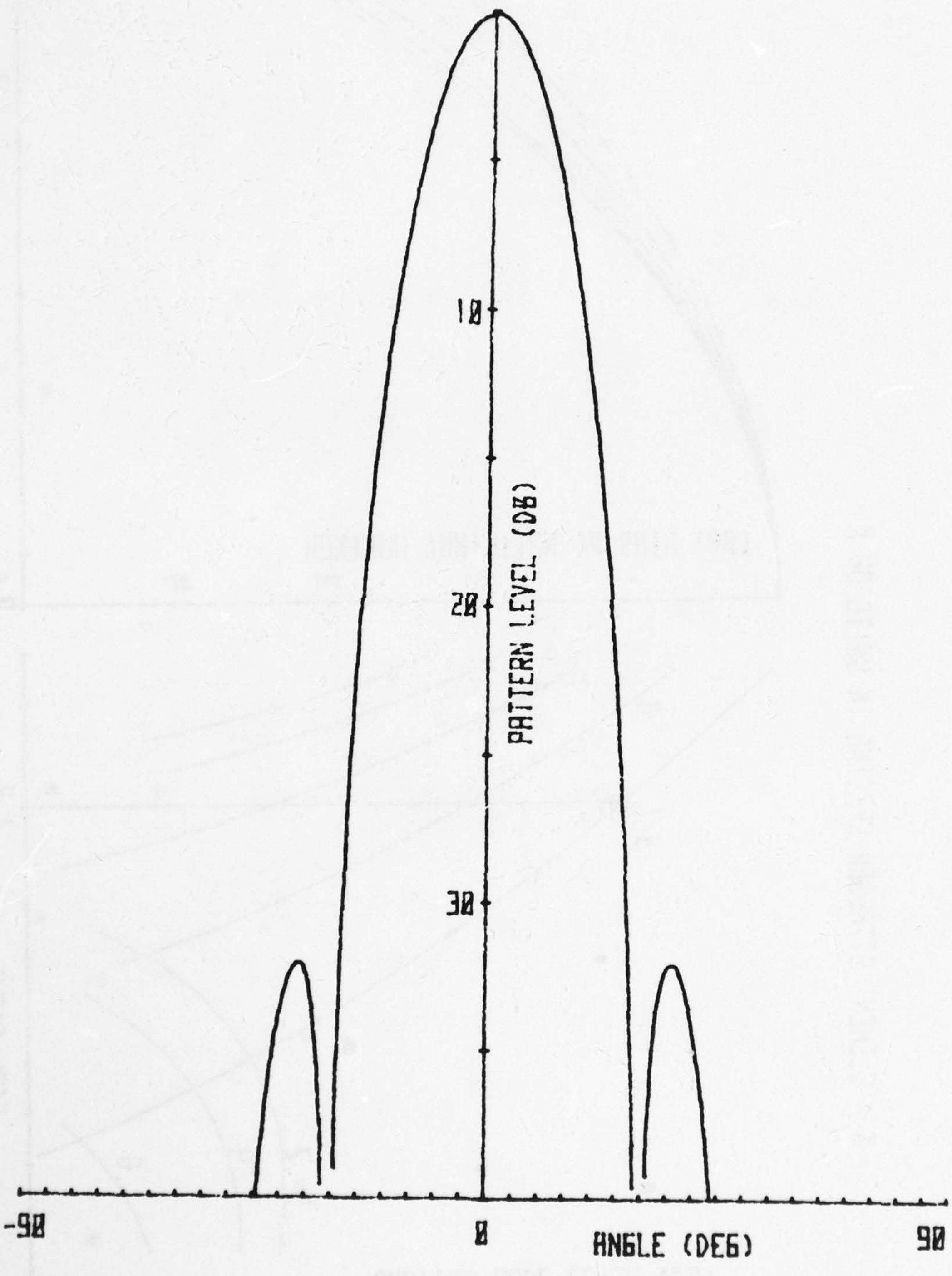

FIG. III.18 AVERAGE STAGGERED 2 PORT PATTERNS

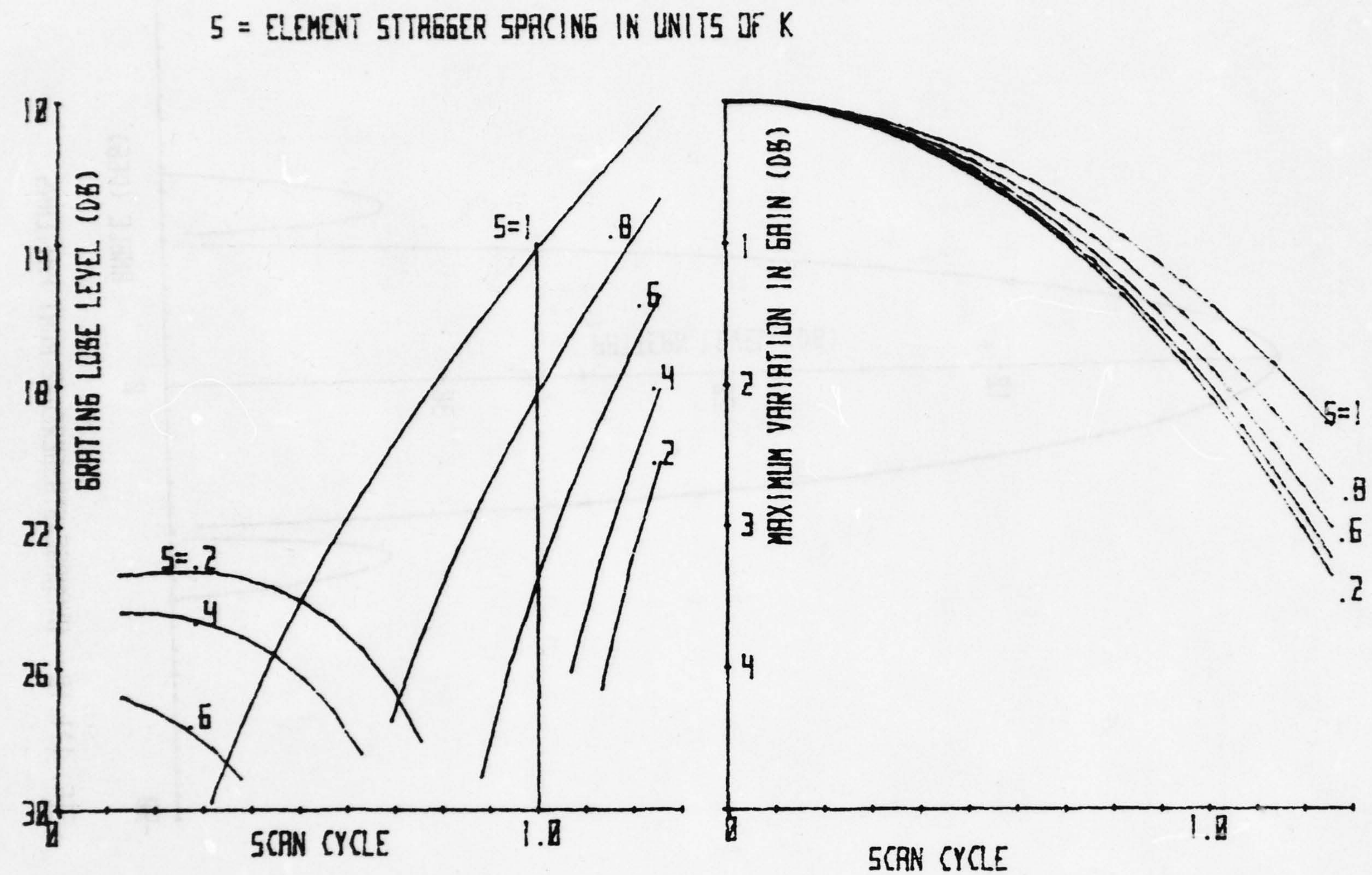

FIG. III.19 GAIN AND GRATING LOBE LEVEL VS. STAGGERED ELEMENT SPACING

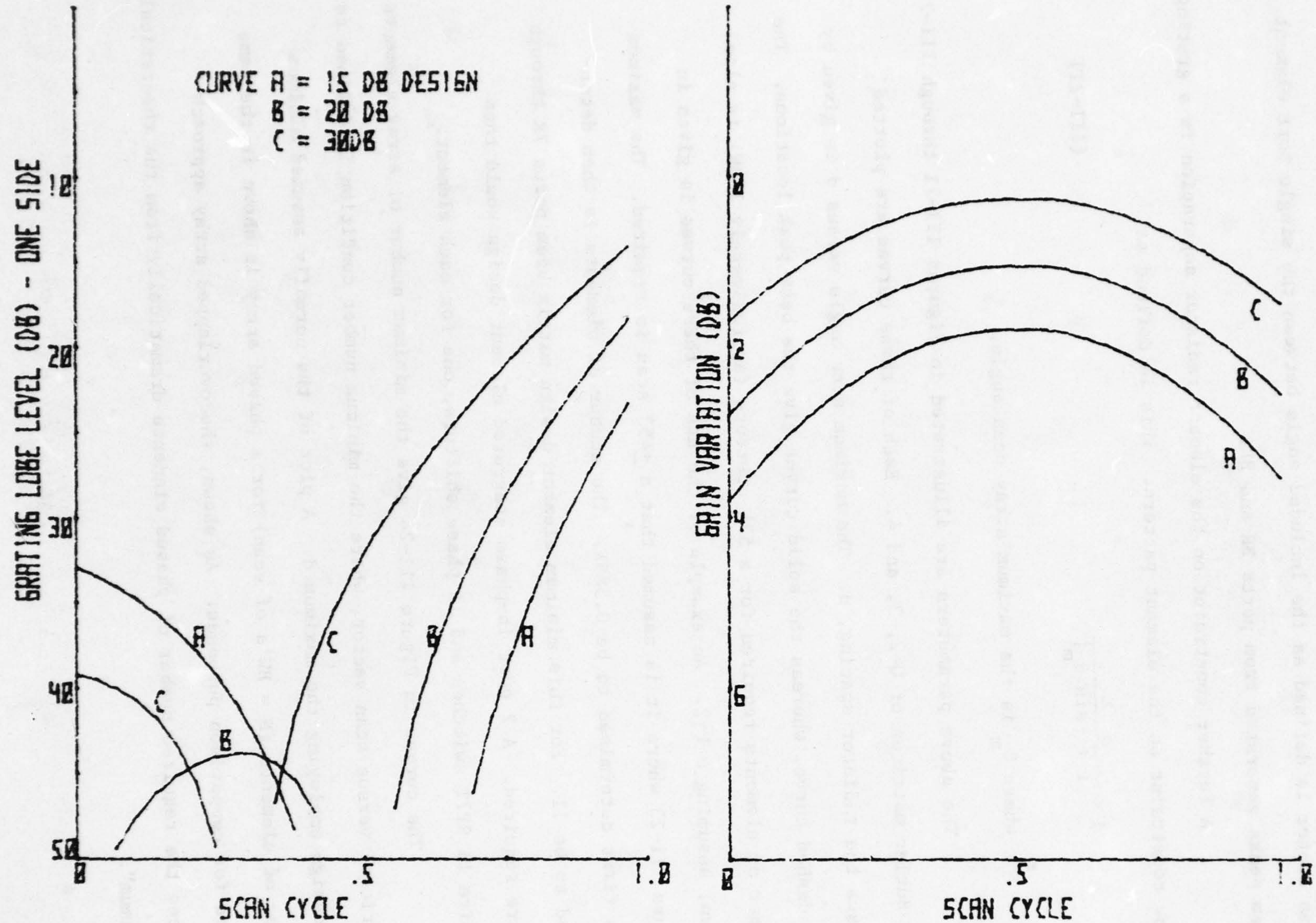

FIG. III.20 GAIN AND GRATING LOBE LEVEL FOR STAGGERED TCHEBYSCHEFF ELEMENTS

Scan sector is defined as the included angle between the single port element beam peaks generated from ports BR and BL.

A further constraint on the element radiator separation is a grating lobe constraint on the element pattern. This is defined as

$$d < \frac{\lambda}{1 + |\sin \theta_m|} \qquad \text{(III-21)}$$

where θ_m is the maximum array scan angle.

The above parameters are illustrated in Figures III-21 through III-23 for Butler matrices of Q=2, 3, and 4. Each of these curves are plotted versus the radiator spacing, d. The maximum scan angle versus d is given by the dashed curve, whereas the solid curves give the beam peak locations. The number of elements required for a 57λ aperture (approximately 1°BW) is also shown, assuming a P=2. An example of the use of these curves is given in Figure III-23 where it is assumed that a ±45° scan is required. The maximum d is first determined to be 0.585λ. The number of elements is then determined to be 11. For this minimum element design matrix beam ports 7R through 7L are required. A 2 port in-phase staggered element design would then require 11 SP7T switches and 11 phase shifters, one for each element.

The curves in Figure III-24 give the minimum number of array elements (matrices) versus scan sector, where the minimum number condition is defined as the design employing the maximum d. A plot of the normally assumed minimum number of elements (N = BW's of scan) for a phased array is shown in the same figure for comparison purposes. As shown, the overlapped array approach reduces the required number of phased elements dramatically from the theoretical "minimum".

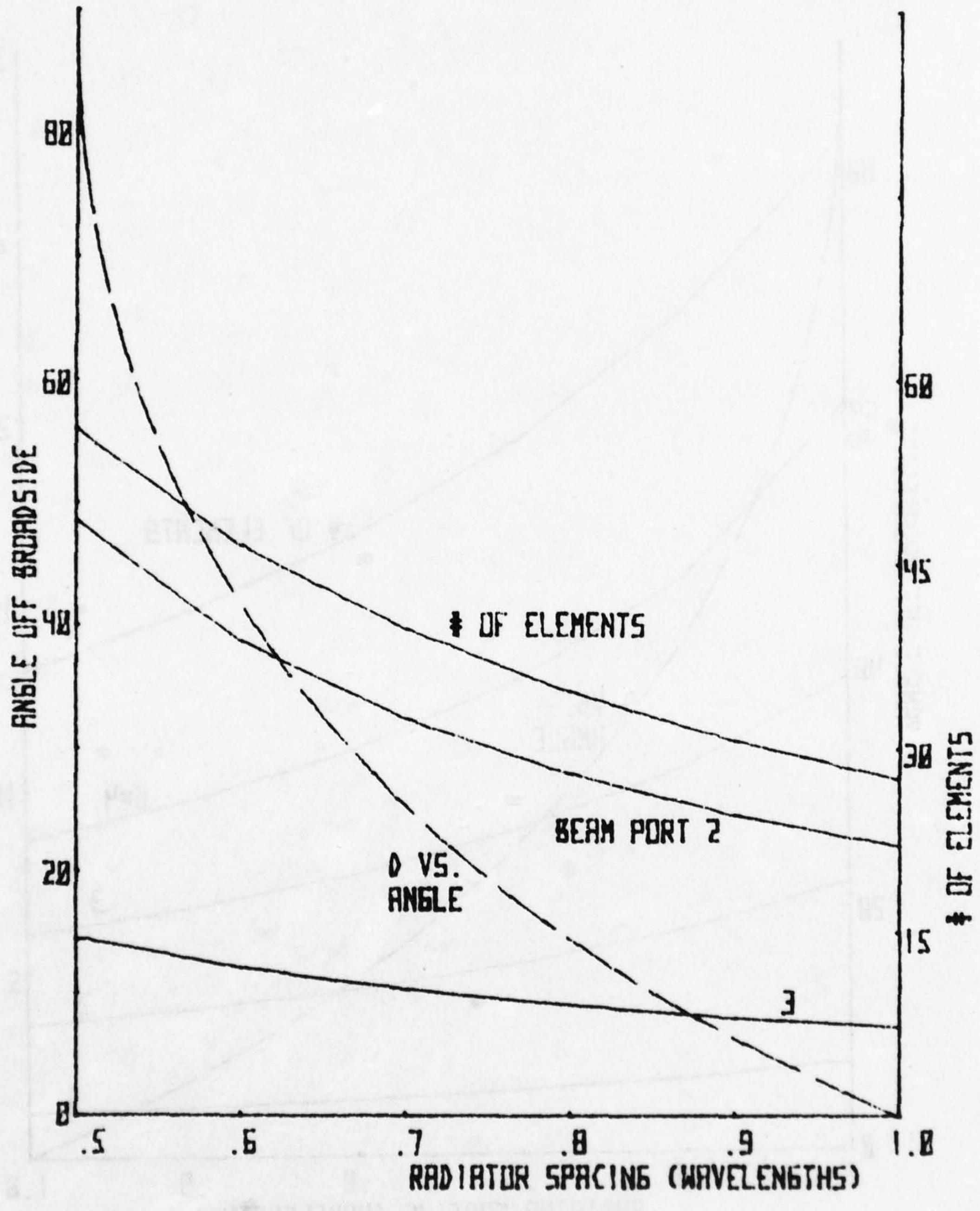

FIG. III.21 4 PORT BUTLER MATRIX ARRAY PARAMETERS

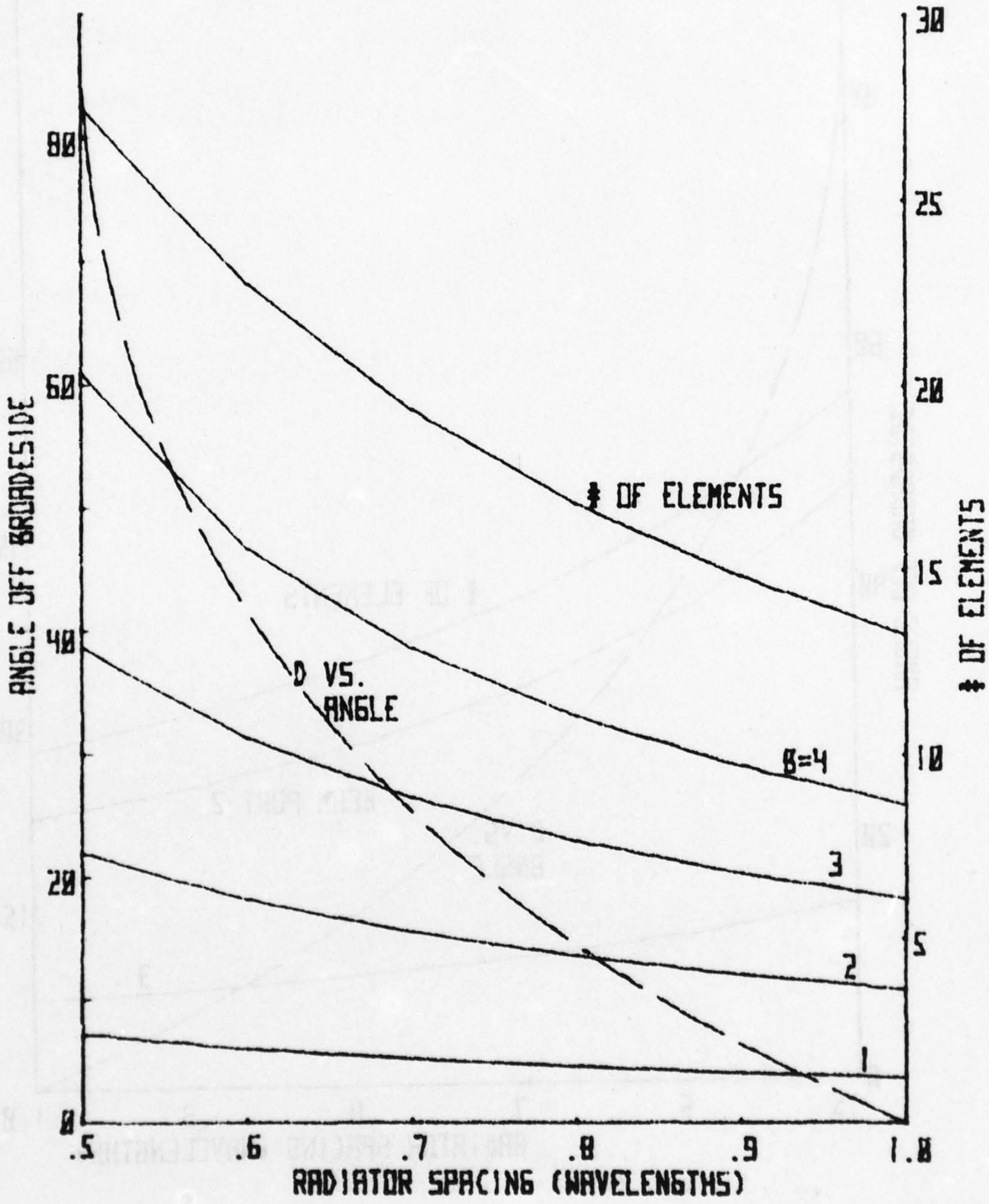

FIG. III.22 8 PORT BUTLER MATRIX ARRAY PARAMETERS

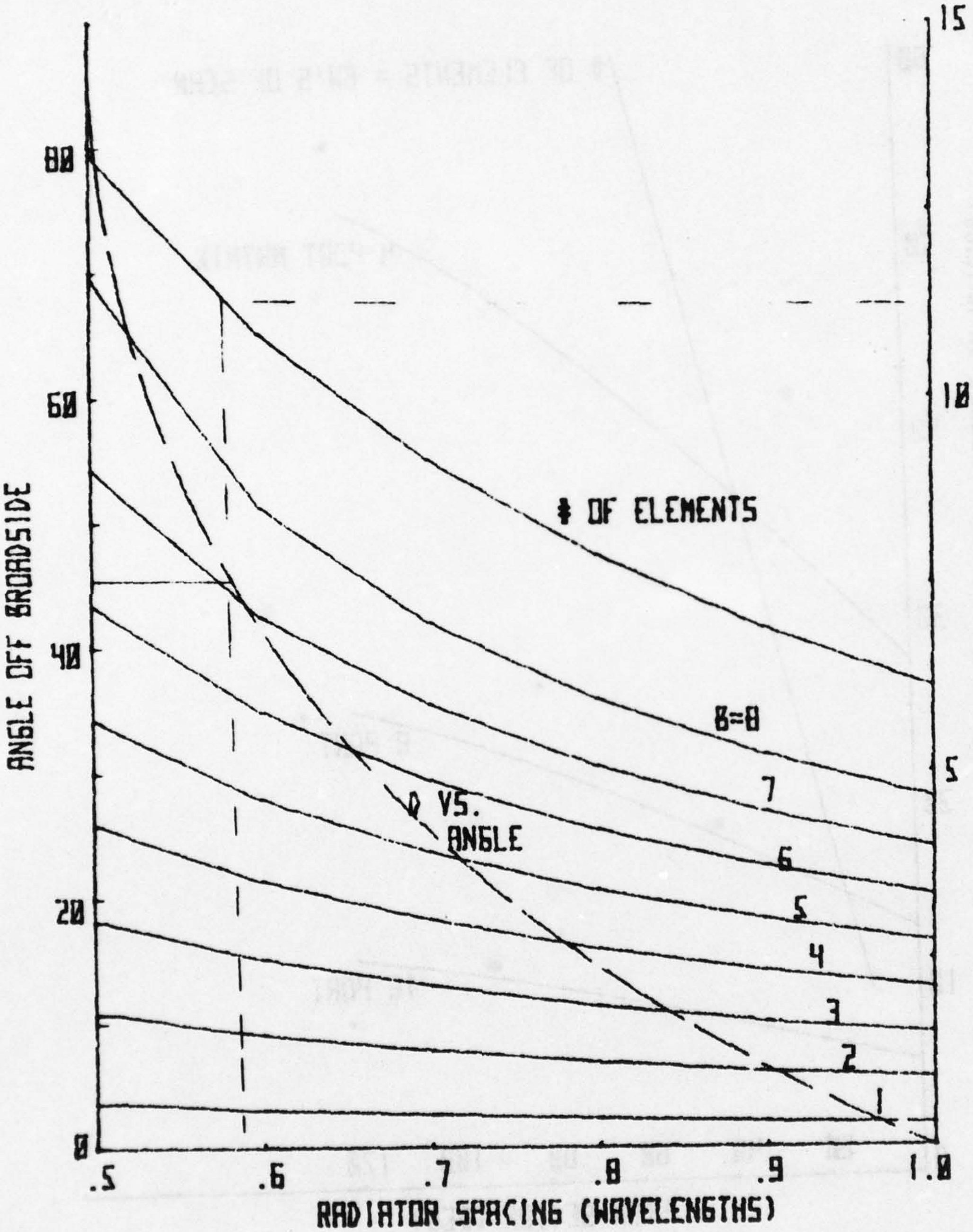

FIG. III.23 16 PORT BUTLER MATRIX PARAMETERS

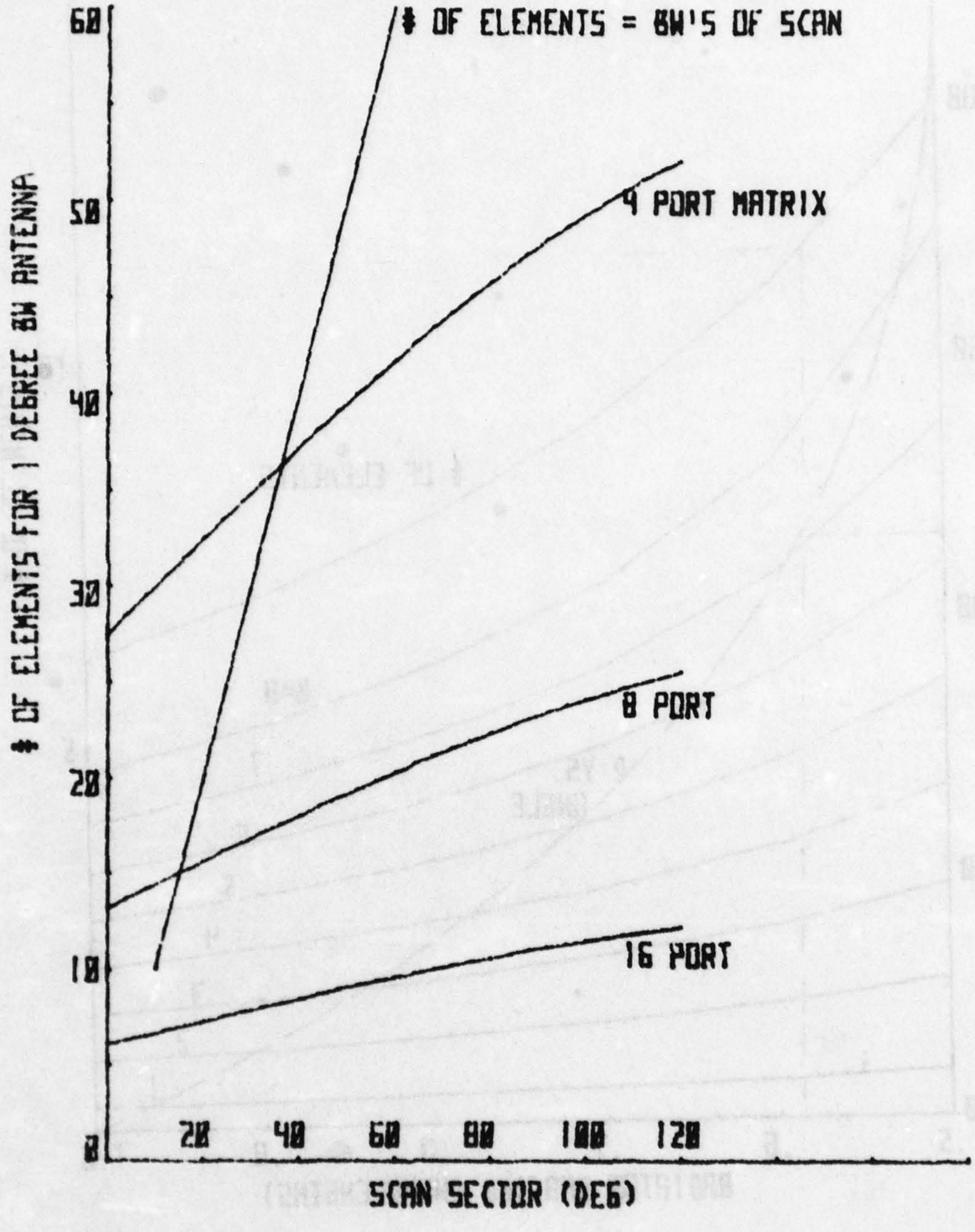

FIG. III.24 MINIMUM NUMBER OF ARRAY ELEMENTS VS. SCAN SECTOR

The Bulter Matrix has wide bandwidth; standard units provide up to an octave bandwidth*. However, since the matrix is not a true time delay network (see reference 2 for networks that are true time delay types), the pointing direction of the single port beam varies with frequency. This change in location can be estimated directly from the beam location curves plotted in Figures III-21 through III-23, since a frequency change can be interpreted as a change in radiator spacing d.

---

* Sanders Associates, Inc., TA-500 Series

IV. ARRAY PERFORMANCE

As discussed in the previous section, there are trade offs to be made between performance and simplicity and/or cost. The arrays selected for computer simulation are based upon simplicity, fewest numbers of components, and presumably low cost. Better pattern performance at the expense of some additional hardware is possible and can be extrapolated from the analysis done in this study. This is discussed in the following sections.

4.1 Limited Scan Array

The simplest useful element pattern is the 2 port in-phase (cosine illumination) pattern. For a minimum circuitry approach for multiple sector operation, the array design would utilize the staggered element pattern approach, i.e., each element stepped at $\sin^{-1}(\frac{2\lambda}{A})$. The trade offs for $\pm$ 10° scan of a one-degree beam are indicated in Table IV-1. The total number of active components are presented in the table along with the number of matrix port positions on the SPMT switch (when M=1, no switch is required and a power divider can be substituted for the matrix). Two values of M are tabulated representing the number of switch positions on each half of the array.

The 2 port in-phase element pattern is a simple, efficient (-0.9 dB) element*. When staggered as indicated above, the array pattern will exhibit a high (-14 dB) grating lobe at the scan limits. This can be reduced considerably by stepping the elements as $\sin^{-1}(\frac{\lambda}{A})$, but at the penalty of adding additional SP2T switches (Section IV.D). Another possibility is to use staggered Tchebyscheff weighted apertures. Resistive taporing of the matrix radiator ports to achieve this element aperture should reduce the maximum

* When the element is staggered, efficiency is further reduced by 2.1 dB, but gain variation is reduced.

TABLE IV-1

LIMITED SCAN PARAMETERS
MINIMUM NUMBER OF COMPONENTS FOR $\pm 10°$ SCAN - 1°BW

CASE	BUTLER SIZE	ELEMENT SIZE A	# OF PHASE SHIFTERS/MATRICES AND SPMT SWITCHES	M
I	4	3.4λ	33	1
II	8	6	18	1,2
III	16	12.8	8	2,3
IV	32	25.6	4	4,5

grating lobe level (to -20 dB for a 15 dB Tchebyscheff design) at the cost of somewhat higher far-out sidelobe levels. These alternatives were not considered for array pattern computer computation in this study.

To illustrate the effect of the array factor on the final pattern, a uniform and 25 dB Tchebyscheff array distributions were selected for a modified version of Case I in Table IV-1*. The results are indicated in Figure IV.1 through IV.4. The major differences between the two can be seen to be the close-in sidelobes. The element pattern effect on the array pattern is clearly evident, with sidelobes beyond ±25° less than -40 dB. The grating lobe maximum is about -30 dB.

Case II in Table IV-1 was computer simulated to illustrate a minimum element number multiple sector design. In this case, 18 elements are used, 9 using an 8 port Butler Matrix with input ports 1R and 2R combined for one half of the scan cycle and 1L and 1R combined for the other half of the scan cycle. The other 9 elements of the array have a fixed beam that can be implemented with a simple 8:1 divider. A 25 dB Tchebyscheff array distribution was assumed. The patterns for this design are shown in Figures IV.5 and IV.6.

The high grating lobe indicated can be reduced at maximum scan angles by increasing the number of elements and reducing the element size, e.g., reducing the element size from $6\lambda(8 \times .75\lambda)$ to $4.8\lambda(8 \times .6\lambda)$ would lower the maximum grating lobe at 10° scan by about 4 dB at the expense of raising the total number of elements to 22. To reduce the high grating lobe at 0° scan, alternate element pattern types such as discussed above would be required.

---

*35 instead of 33 elements were used allowing slightly smaller radiator spacing of $.8\lambda$ versus $.85\lambda$, thus avoiding a high element and array grating lobe at ±90°.

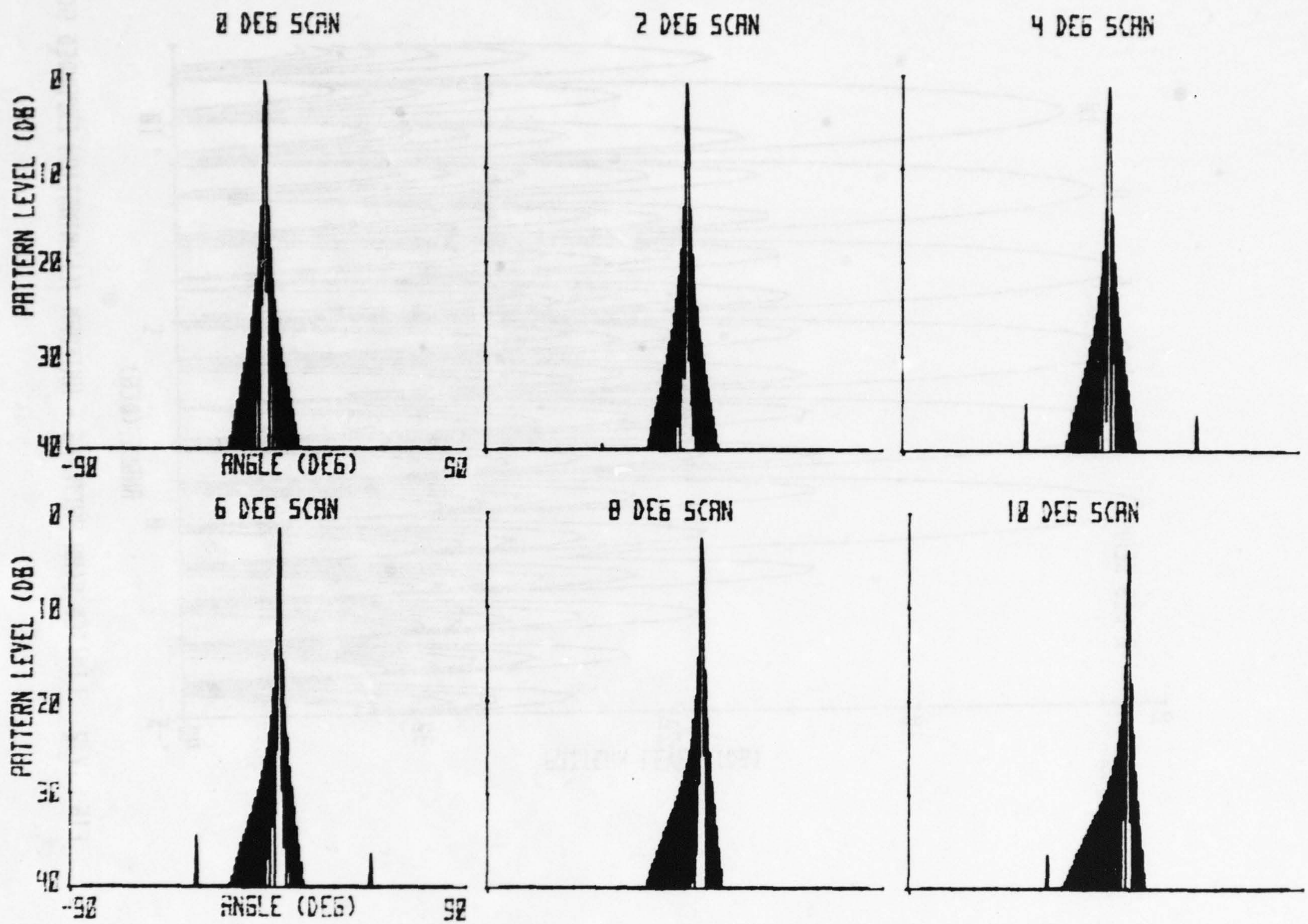

FIG. IV.1 LIMITED SCAN PATTERNS - UNIFORM ILLUMINATION

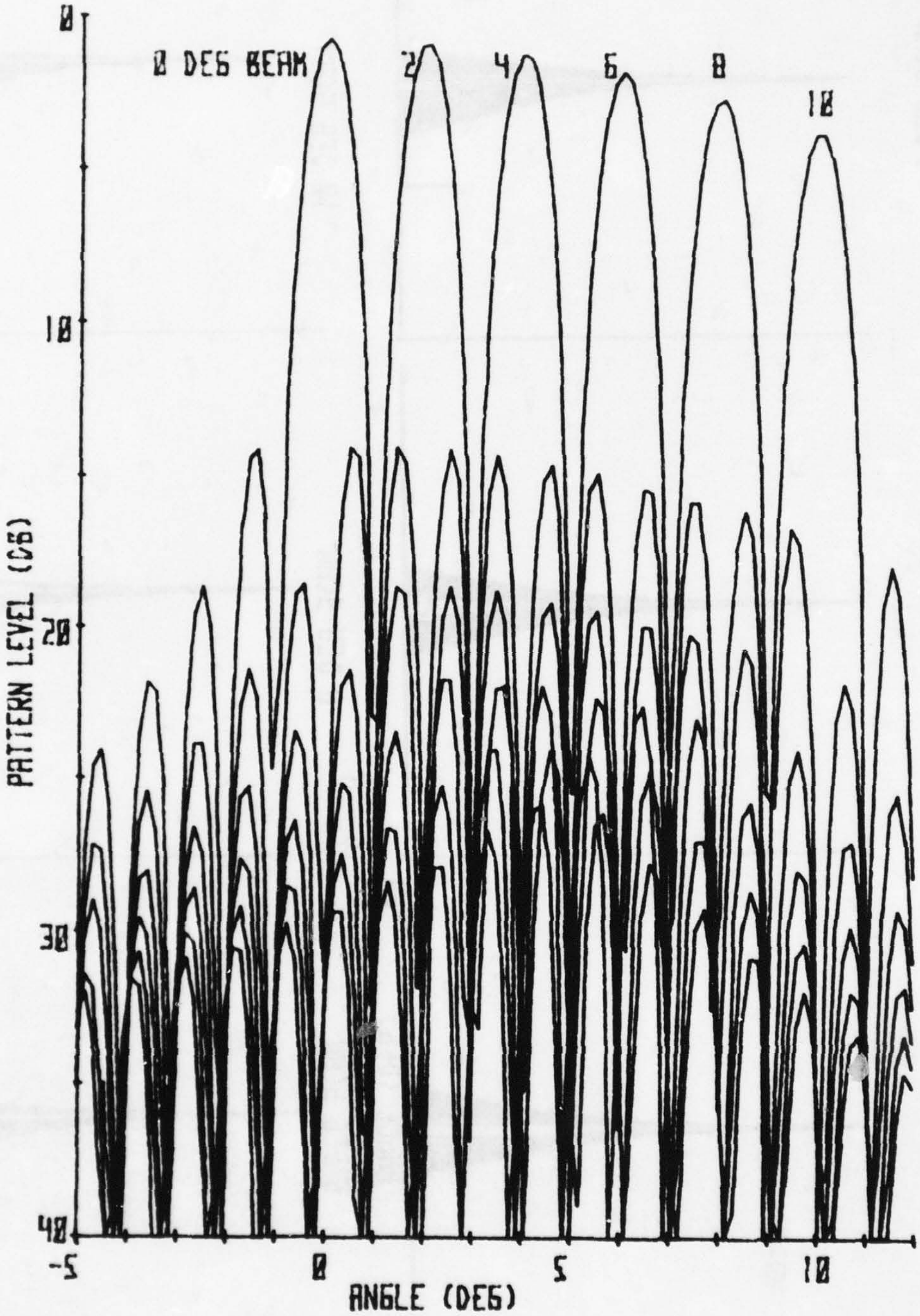

FIG. IV.2 LIMITED SCAN PATTERNS - UNIFORM ILLUMINATION EXPANDED SCALE

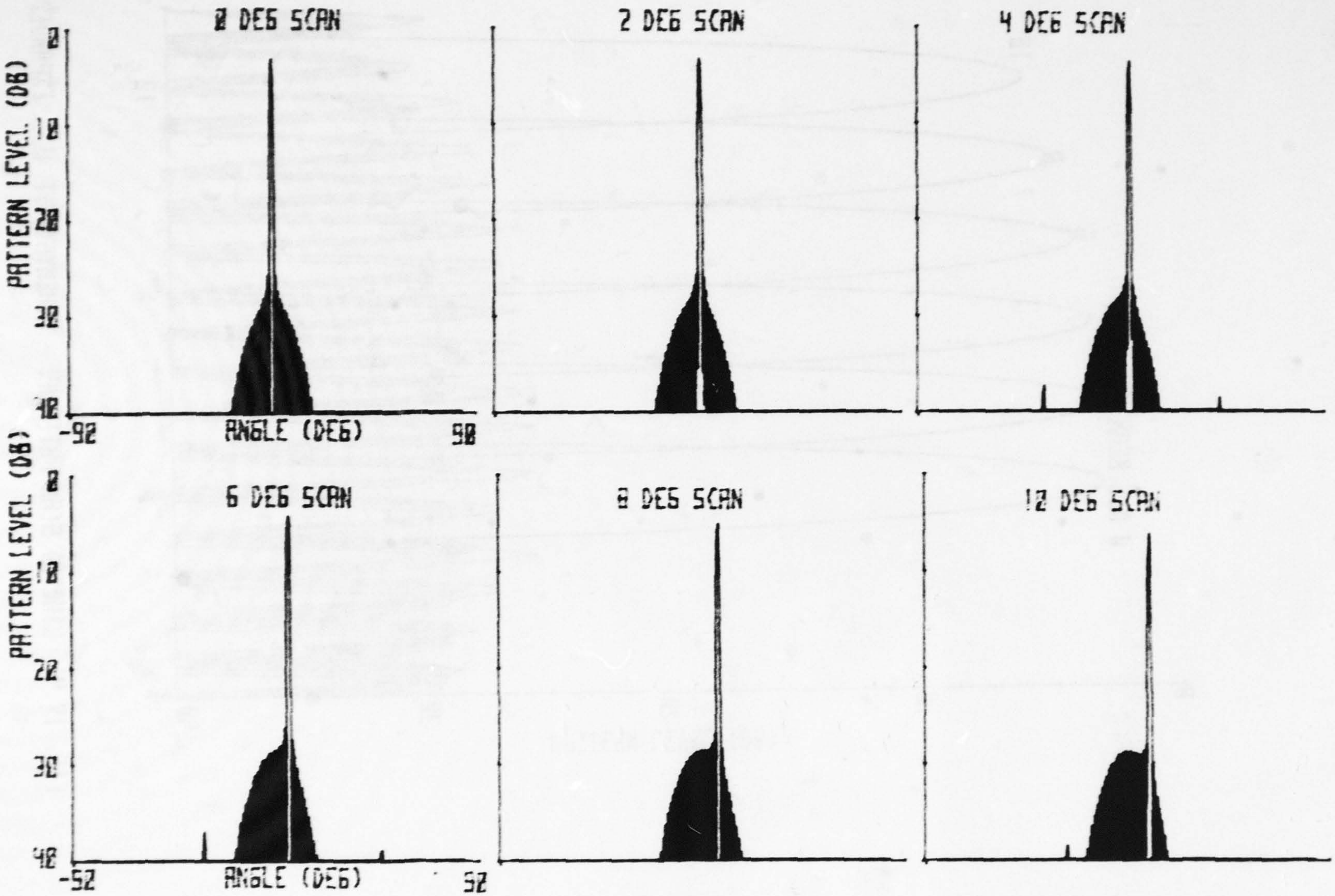

FIG. IV.3 LIMITED SCAN PATTERNS - TCHEBYSCHEFF ILLUMINATION

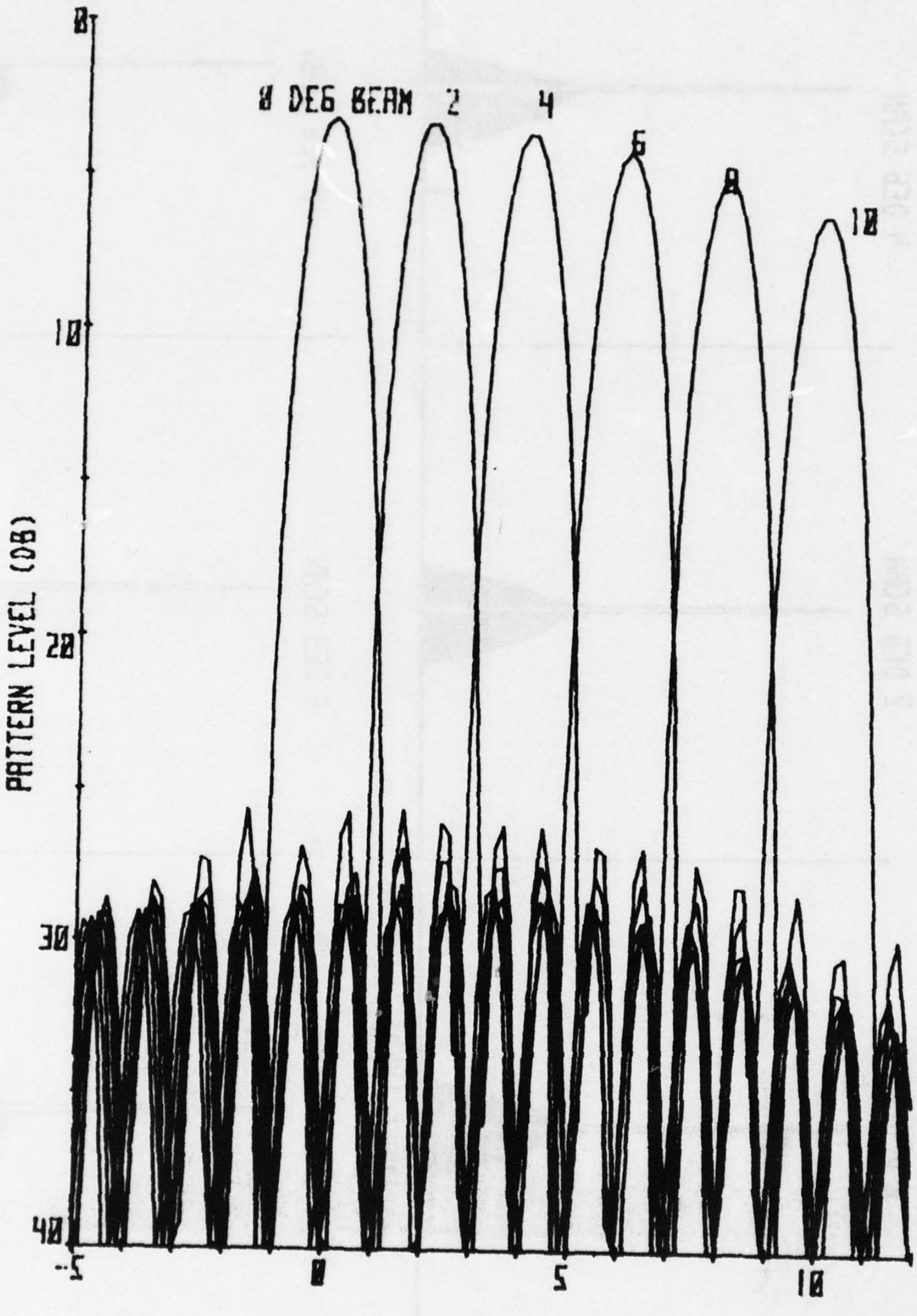

FIG. IV.4 LIMITED SCAN PATTERNS - TCHEBYSCHEFF ILL. EXPANDED SCALE

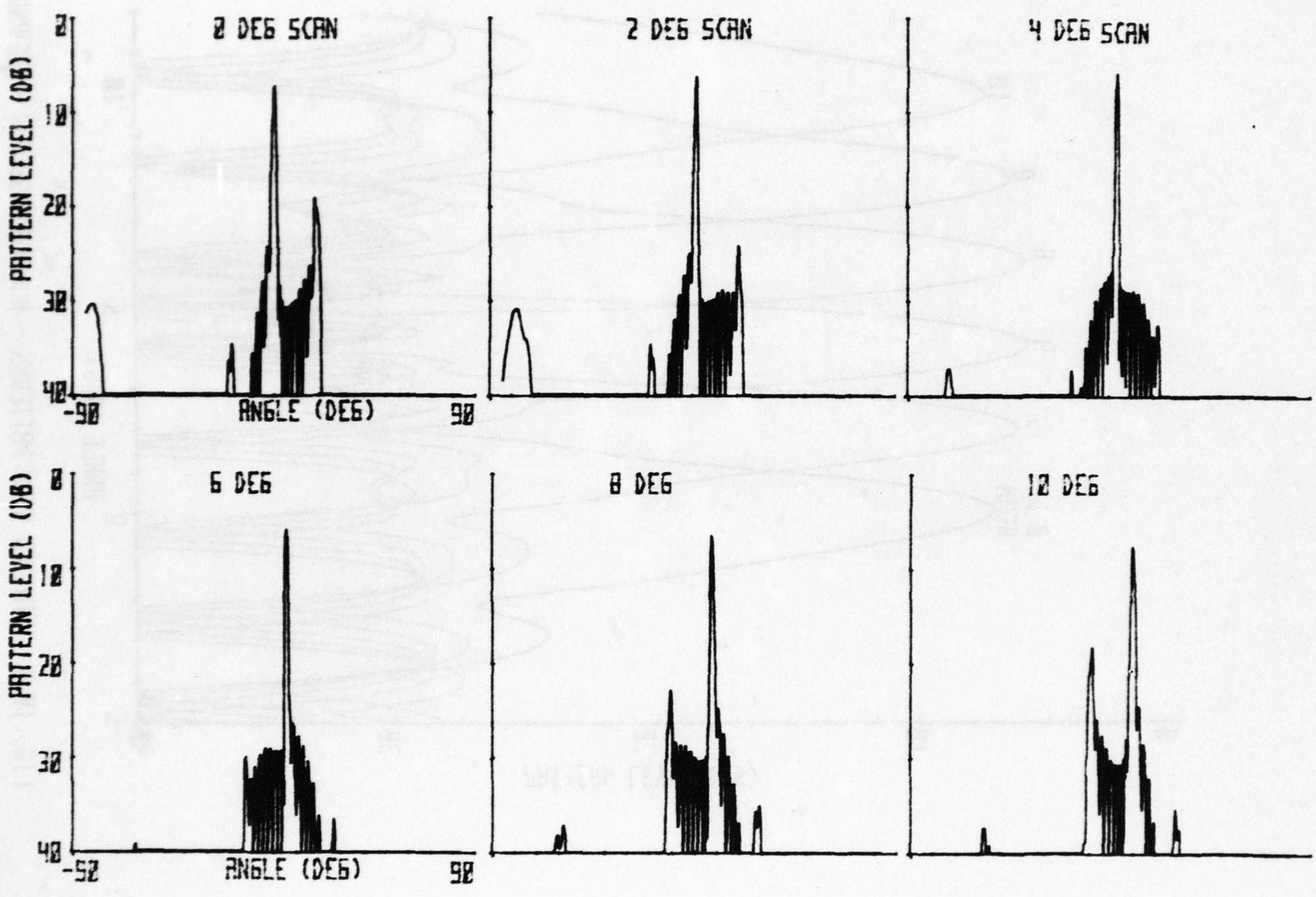

FIG. IV.5 LIMITED SCAN PATTERNS - MULTIPLE SECTOR

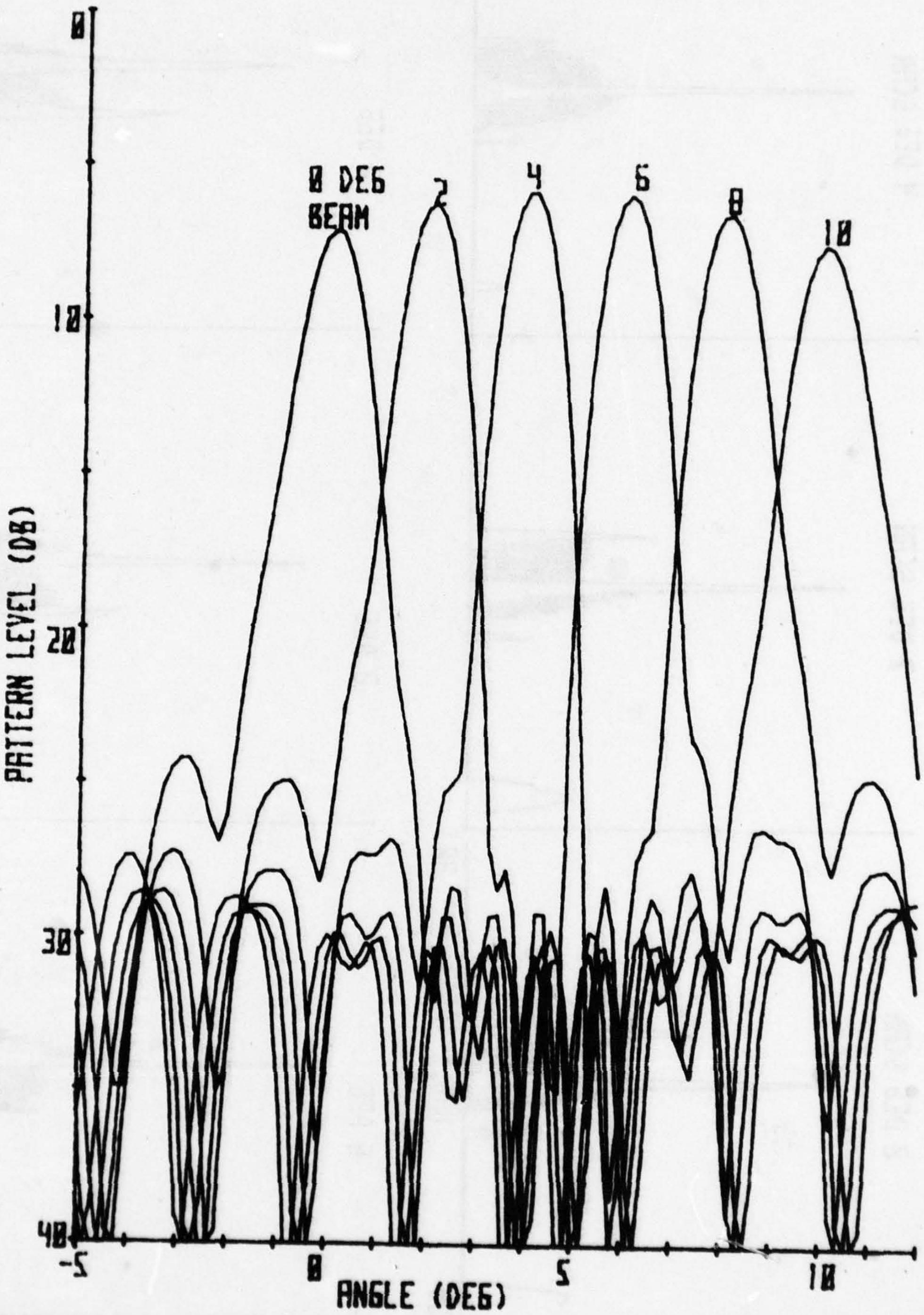

FIG. IV.6 LIMITED SCAN PATTERNS - MULTIPLE SECTOR - EXPANDED SCALE

4.2 Wide Angle Scan

The tradeoffs for a minimum component design of a 1°BW ±45° scan antenna are indicated in Table IV-2. As in the case of the limited scan design, only staggered element patterns are assumed, with each element pattern being a 2 port in-phase Butler Matrix type. The options available for pattern performance improvement discussed in Section 4.1 apply as well to the wide angle scan design.

A modification of Case II in Table IV-2 was taken for computer simulation. The number of elements was increased by one to 26 and both a .5λ and .55λ radiator spacing design considered. The two radiator spacings correspond to operation at two frequencies over a 10% band. Half the elements use 6 of the input matrix ports and have a SP3T switch selecting 3 possible beam positions. The other half of the array uses all 8 ports and a SP4T switch per element. A 25 dB Tchebyscheff distribution is assumed.

The .5λ radiator design patterns are shown in Figures IV.7 through IV.9. The .55λ radiator design patterns are very similar to those for the .5λ spaced radiators. The major differences occur in the amplitude of the array beam at a given angle since the element pattern peak shifts as much as 5.6° for the extreme angular sectors. For simultaneous wideband operation, this would represent a gain versus frequency variation but no beam pointing error if the matrix elements phase shifters were true time delay devices. The .55λ spaced array results are illustrated in Figure IV.9.

The directivity of these patterns, as determined through computer integration of the simulated patterns, is 19.7 dB to 18.3 dB. Theoretical

TABLE IV-2

WIDE ANGLE SCAN PARAMETERS
MINIMUM NUMBER OF COMPONENTS FOR ± 45° SCAN -1°BW

CASE	BUTLER SIZE	ELEMENT SIZE A	# PHASE SHIFTERS/MATRICES AND SPMT SWITCHES	M
I	4	2.2	50	2,3
II	8	4.4	25	3,4
III	16	8.8	12	6,7
IV	32	17.6	6	13,14

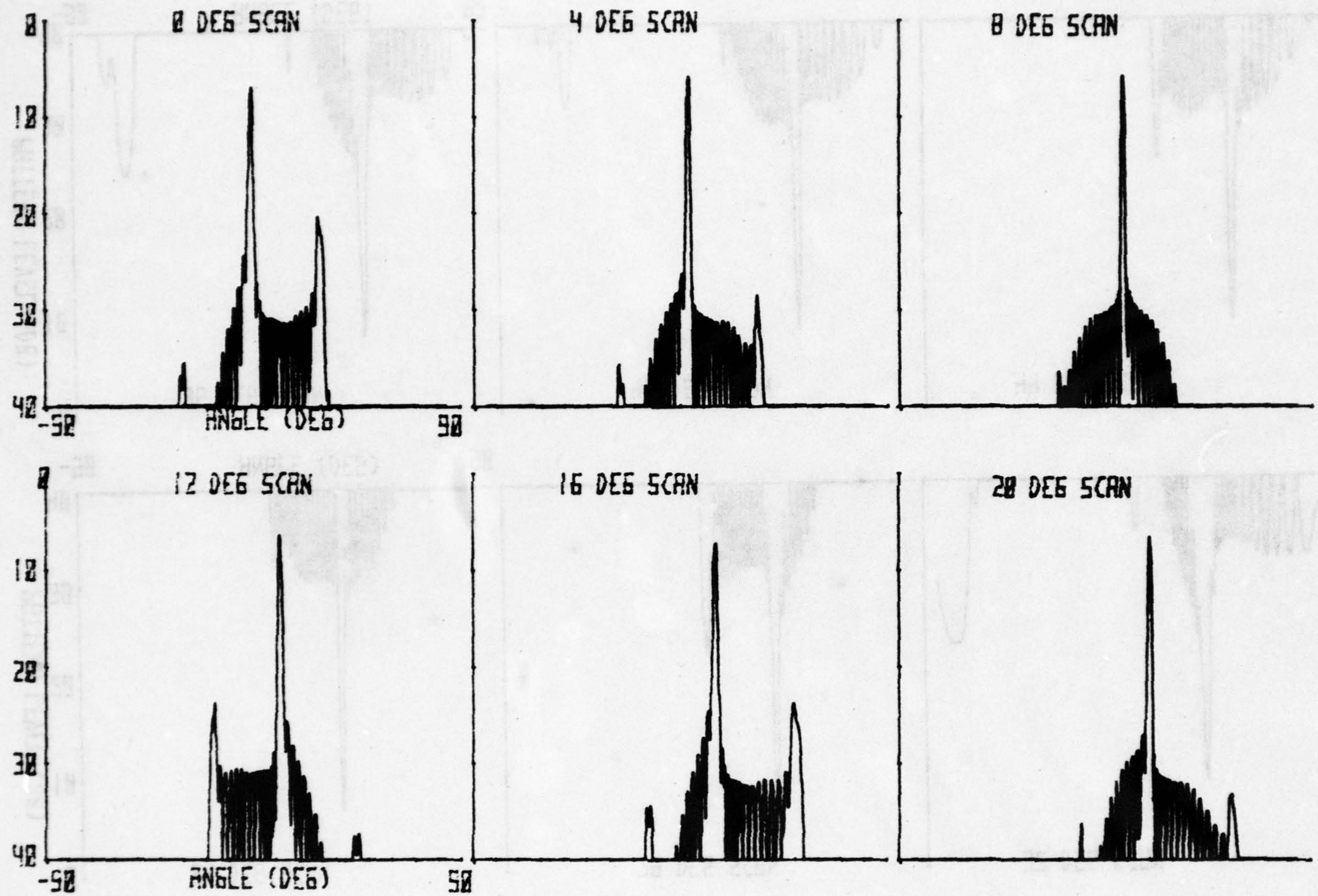

FIG. IV.7 WIDE ANGLE SCAN PATTERNS

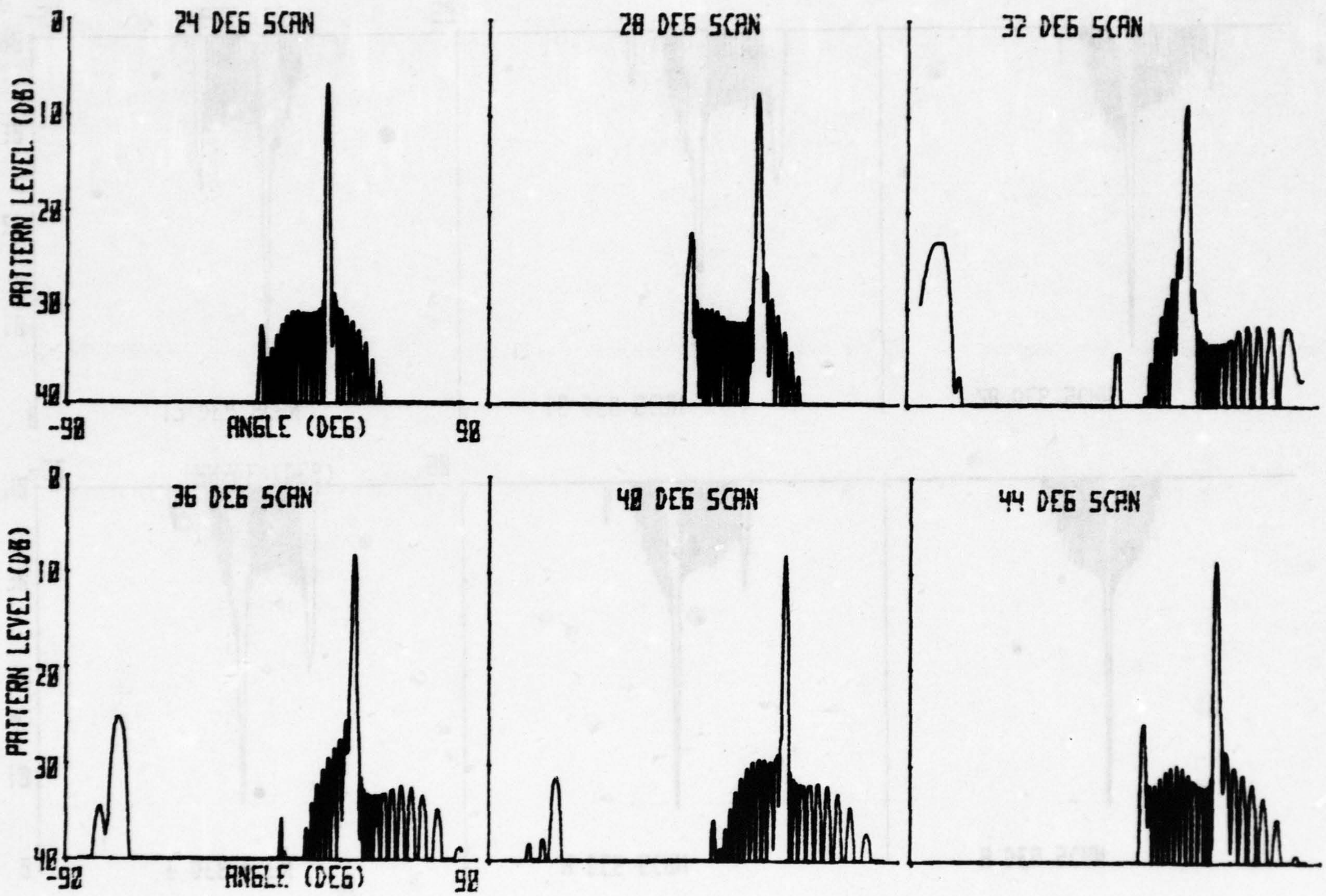

FIG. IV.8 WIDE ANGLE SCAN PATTERNS CONTINUED

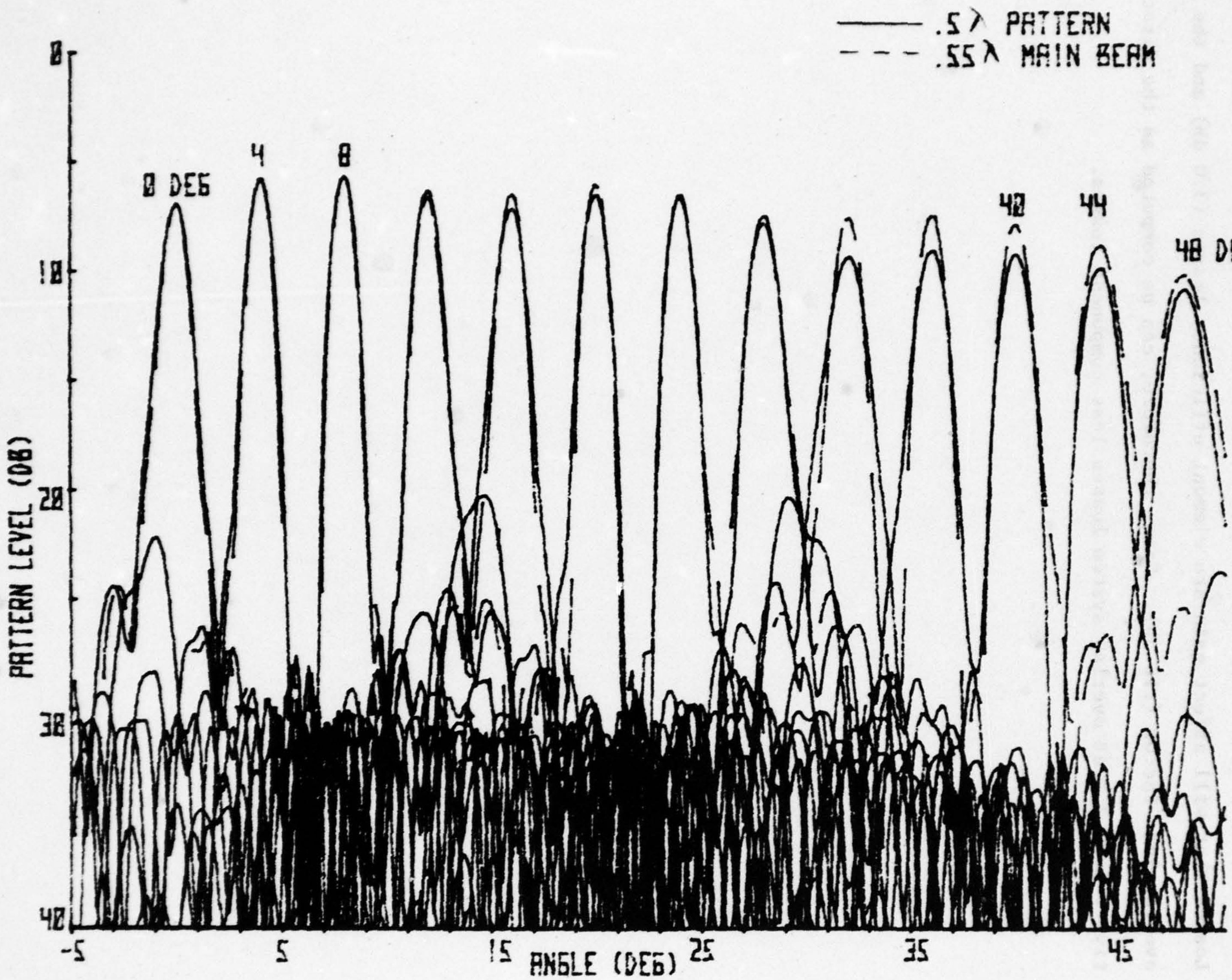

FIG. IV.9 WIDE ANGLE SCAN PATTERNS - EXPANDED SCALE maximum directivity is 20.1 dB. With an expected gain variation of 1.5 dB due to the element factor shape, the expected directivity is 20.1 dB to 18.6 dB. Losses that will affect gain are element efficiency losses (3.0 dB) and the overlap loss factor (.16 dB). Gain, therefore, can be computed as the directivity less 3.2 dB overlap system losses less component losses.

V. COMPONENT TRADE OFFS

Trade off of design parameters to achieve a given cost objective with maximum performance or a given performance level at lowest cost is very much a function of the detail specifications. Therefore, only a general discussion of the parameter selections can be presented. This hopefully would narrow the range of parameters that would be considered for a given requirement.

Discussion of the performance versus the number of elements, overlap factor, element pattern, Butler Matrix size, and element beam step was discussed in Sections III and IV. The relationship of these parameters to cost and reliability is now of interest. The basic components are: 1) the matrix feeds, 2) phase shifters, and 3) the switches.

Matrix

Butler matrices up to 64 ports have been manufactured with good performance. The networks are all passive multiple layer printed circuits that are low cost unless they get physically very large. At microwave frequencies, matrices equalling to 16 ports or less appear reasonable in size and cost. This does not appear to be restrictive as larger networks tend to result in too many scan sectors (SPMT switches with M large) or too few phase shifters for effective pattern control.

Since the number of elements is inversely proportional to the element aperture, it is also inversely proportional to the matrix size. Therefore, going from an 8 port matrix to a 16 port matrix will halve the number of matrices required. Matrix reliability (very high) has not changed. The cost of the individual matrix, however, has increased by about a factor of 2.5*.

---

*From discussion with Sanders Associates, Inc.

The absolute cost of an 8 port Butler Matrix in production quantities is not readily available. However, estimates would place it in the range of two times the cost of a 4-bit phase shifter.

Phase Shifters and Switches

A 4-bit phase shifter (assumed to be required for a typical design) has the same number of the same type diodes as a SP4T switch. Furthermore, the circuit construction is very similar. Therefore, it would be reasonable to assume comparable costs for these two items.

The drivers for the two devices and the input logic is different. Furthermore, as the number of phase shifters are reduced at the cost of increased switch positions, the beam steering logic is greatly simplified as is the cabling. As a first-order estimate, we might consider the cost of SP4T switches and 4-bit phase shifters to be equal.

If one were to take the above cost relations for the matrix and switches and normalize them to a 4-bit phase shifter, and assume M is proportioning to matrix size, the cost for an 8 port Butler system and a 16 port Butler system would be about the same, or

$$\frac{\text{cost}}{\text{cost of phase shifter}} = N(3 + \frac{M}{4})$$

where M is the number of switch positions and N is the number of elements required for an 8 port matrix design.

VI. CONCLUSION AND DISCUSSION

The phased array technique using an overlapped multiple-beam element has been investigated and relations between parameter selection and performance established. Two designs, one for limited scan and phase shifters was selected for computer analysis. The results indicated ultra low sidelobe levels are possible over most of the angular sector while limiting the close in sidelobes to no more than -20 dB and grating lobe levels to peak values of about -14 dB for a few scan locations. The wide angle design provides 90 beamwidths of scan (1° BW scanned ± 45°) with (26) 8 port Butler Matrix elements, (26) phase shifters, and (26) SP4T switches. The limited scan design utilizes (18) 8 port matrices, 18 phase shifters, and (9) SP2T switches to achieve 20 BW's of scan.

Analysis indicates pattern performance can be further improved at the cost of additional elements and element complexity. The technique, therefore, would appear to have wide application for receive and transmitting systems. Two dimension scan can be visualized as a straightforward extrapolation of the described technique where it is used as the row and column scanning networks for a row-column phased array.

The short study reported on represents only an initial look at the possibilities of this new array technique. Further analysis is called for in the following areas:

A. Techniques

1. Alternate type elements - lens and matrices
2. Higher order overlap factors
3. Wideband signal design requirements

B. Systems

1. Two dimension scanning
2. Designs for high performance applications, e.g., ultra low sidelobe designs
3. Multiple-beam array designs.

Additional analysis is also called for in the area of reliability, monitoring, and cost for arrays that operate with very few elements.

REFERENCES

1. Stein, "Cross Coupling on Multiple-Beam Antenna," PGAP, (September 1962) 548-557.

2. R. C. Hansen, "Microwave Scanning Antennas," III, Chapter 3, Section III, Academic Press (1966).

MISSION
of
Rome Air Development Center

RADC plans and executes research, development, test and selected acquisition programs in support of Command, Control Communications and Intelligence (C^3I) activities. Technical and engineering support within areas of technical competence is provided to ESD Program Offices (POs) and other ESD elements. The principal technical mission areas are communications, electromagnetic guidance and control, surveillance of ground and aerospace objects, intelligence data collection and handling, information system technology, ionospheric propagation, solid state sciences, microwave physics and electronic reliability, maintainability and compatibility.

**Printed by
United States Air Force
Hanscom AFB, Mass. 01731**